

Accepted Manuscript

Design, Synthesis and Biological Evaluation of Novel Pyrazoline-Containing Derivatives as Potential Tubulin Assembling Inhibitors

Ya-Juan Qin, Yu-jing Li, Ai-Qin Jiang, Meng-Ru Yang, Qi-Zhang Zhu, Hong Dong, Hai-Liang Zhu



PII: S0223-5234(15)00154-3

DOI: [10.1016/j.ejmech.2015.02.058](https://doi.org/10.1016/j.ejmech.2015.02.058)

Reference: EJMECH 7740

To appear in: *European Journal of Medicinal Chemistry*

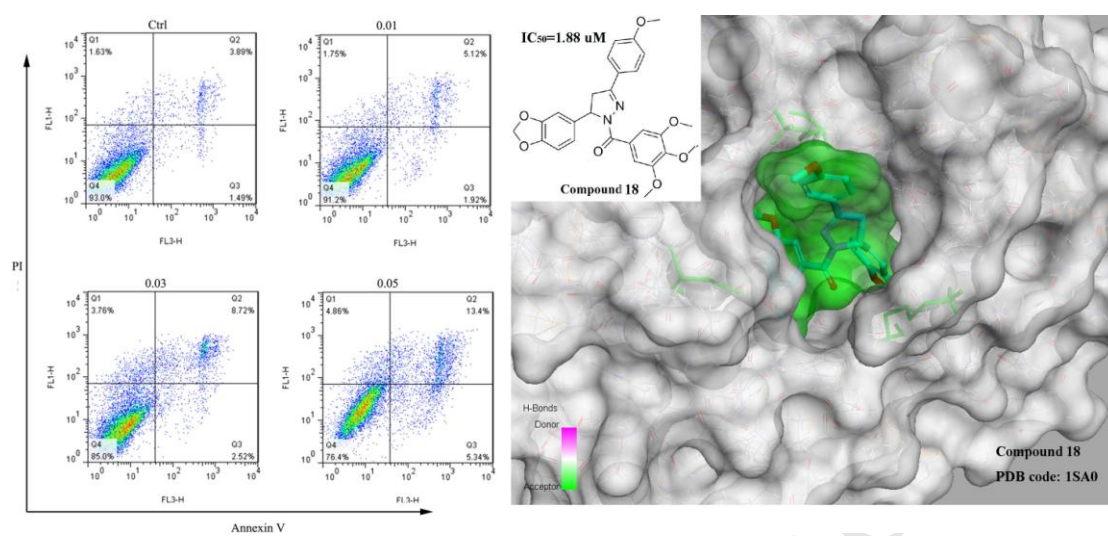
Received Date: 11 August 2014

Revised Date: 5 November 2014

Accepted Date: 28 February 2015

Please cite this article as: Y.-J. Qin, Y.-j. Li, A.-Q. Jiang, M.-R. Yang, Q.-Z. Zhu, H. Dong, H.-L. Zhu, Design, Synthesis and Biological Evaluation of Novel Pyrazoline-Containing Derivatives as Potential Tubulin Assembling Inhibitors, *European Journal of Medicinal Chemistry* (2015), doi: 10.1016/j.ejmech.2015.02.058.

This is a PDF file of an unedited manuscript that has been accepted for publication. As a service to our customers we are providing this early version of the manuscript. The manuscript will undergo copyediting, typesetting, and review of the resulting proof before it is published in its final form. Please note that during the production process errors may be discovered which could affect the content, and all legal disclaimers that apply to the journal pertain.



Design, Synthesis and Biological Evaluation of Novel Pyrazoline-Containing Derivatives as Potential Tubulin Assembling Inhibitors

**Ya-Juan Qin^{a†}, Yu-jing Li^{a†}, Ai-Qin Jiang^{b*}, Meng-Ru Yang^a, Qi-Zhang Zhu^a,
Hong-Dong^{a*}, Hai-Liang Zhu^{a*}**

^a *State Key Laboratory of Pharmaceutical Biotechnology, School of Life Science, Nanjing University, Nanjing 210093, P. R. China*

^b *School of Medicine, Nanjing University, Nanjing 210093, P. R. China*

[†] Both authors contributed equally to this work.

Abstract

A series of novel pyrazoline-containing derivatives (**15-47**) has been designed, synthesized and evaluated for their biological activities. Among them, compound **18** displayed the most potent antiproliferative activity against A549, MCF-7 and HepG-2 cells line ($IC_{50} = 0.07 \mu M$, $0.05 \mu M$, $0.03 \mu M$, respectively) and the tubulin polymerization inhibitory activity ($IC_{50} = 1.88 \mu M$), being comparable to CA-4. Furthermore, we also tested that compound **18** was a potent inducer of apoptosis in HepG-2 cells and it had cellular effects typical for microtubule interacting agents, causing accumulation of cells in the G2/M phase of the cell cycle. [These studies, along with molecular docking, provided a new molecular scaffold for the further development of antitumor agents that target tubulin.](#)

Keywords: tubulin polymerization inhibitors; pyrazoline; molecular docking

Abbreviations: CA-4, combretastatin A-4; SAR: structure-activity relationship; IC_{50} , half maximal inhibitory concentration; MTT, 3-(4, 5-Dimethylthiazol-2-yl)-2, 5-diphenyltetrazolium bromide

*Corresponding authors. Tel: +86-25-8359 2572; Fax: +86-25-8359 2672.

E-mail address: zhuhl@nju.edu.cn

Introduction

Microtubules are cytoskeletal structures [1] and critical elements in various fundamental cellular processes such as cell division, formation, and maintenance of cell shape, motility, cell signaling, secretion, and intracellular transport. [2] This is one of the reasons why microtubules are an attractive target for anticancer agents. So far, microtubule-targeting agents could be simply classified into microtubule stabilizer and microtubule destabilizer according to the mechanism by interfering with microtubule dynamics. Further divided, there are four major binding sites provided by the microtubule: the taxane site and the laulimalide/peloruside A site for microtubule stabilizer, and the vinca site and the colchicine site for microtubule destabilizer. [3, 4]

In the last decade years, there has been a continuous interest in the exploitation of novel small molecules which are able to inhibit tubulin polymerization. Compound **1** (Combretastatin A-4) [5, 6] (CA-4, **Figure 1**), isolated from the bark of the South African tree *Combretum caffrum*, [7] is one of the prominent tubulin-binding molecules by affecting microtubule dynamics. CA-4 strongly inhibits the tubulin polymerization by binding to the colchicine site of the tubulin. [8] Other natural products such as compound **2** (Colchicine) [9] (**Figure 1**), compound **3** (Podophyllotoxin) [9, 10] (**Figure 1**) and compound **4** (Steganacin) [9] (**Figure 1**) exhibit potent tubulin polymerization inhibitory activity by binding to the colchicine binding site and their distinctive structural features play a fundamental role in the design of tubulin polymerization inhibitors. *Analysis of these microtubule inhibitors indicates that the 3, 4, 5-trimethoxyphenyl groups seem to play an important role in their bioactivity.* *Cis*-olefin configuration at the bridge of CA-4 has been reported as prerequisites for the activity of potent anti-tubulin polymerization. [11] *Cis* configuration of CA-4 is prone to isomerize to transform during storage and administration, which produces a dramatic reduction in the anti-tubulin activity. [12] Therefore, to retain the *cis*-olefin configuration of CA-4, it has been reported that the isomerization from *cis*- to *trans*-olefin can be avoided by incorporating the double

bond in five-member aromatic heterocyclic rings [12], such as pyrazole,[13] imidazole,[14] thiazole [13] and so on. For example, some synthesized compounds such as compound **5** (CA-NH₂) [15], **6** (A-105972) [8], **7** (A-204197) [16], **8** (SMART) [17], **9** (Pyrazole) [18] and **10** (RABI) [19] (**Figure 1**) also strongly inhibit the tubulin polymerization by binding to the colchicine site of the tubulin. In 2001, compound **6** (A-105972), reported by Abbott, a novel colchicine-site binding agent, was selected for biological profiling from a high throughput screening of more than 60,000 compounds, which was based on inhibition of cell proliferation. [8] Subsequently, Abbott extended their initial observation and reported that compound **7** (A-204197) showed more significant tubulin polymerization inhibitory activity and also showed bioactivity against several MDR positive cell lines. [16] Moreover, we have performed docking simulations using the X-ray crystallographic structure of the tubulin in complex with a tubulin inhibitor (PDB code: 1SA0) to explore the binding modes of these compounds at the active site.

These previous researches and docking simulations encouraged us to design and synthesize compounds **15-47** (**Table 1**) which were pyrazoline-containing derivatives. This combined substructures—the pyrazoline ring along with methylphenyl group—might possess synergistic tubulin inhibitory effect. Some novel potent potential tubulin inhibitors were recently reported as potent anticancer agents targeting tubulin in our group and some had demonstrated potent tubulin inhibitory activity. [11, 20] In order to extend our research, here we describe the synthesis of these target compounds and the ensuing structure-activity relationship (SAR) studies. Biological evaluation indicated that some of the synthesized compounds were potent inhibitors of tubulin polymerization. Molecular Docking simulations were performed using the X-ray crystallographic structure of the tubulin in complex with an inhibitor (PDB code: 1SA0) to explore the binding modes of these compounds at the active site.

2. Results and discussion

2.1. Chemistry

The synthetic route of compounds **15-47** is outlined in **Scheme 1**. Firstly, a solution of 3, 4-dihydroxybenzaldehyde in DMF was added drop wise to a suspension of CH_2Cl_2 and K_2CO_3 in DMF and then we obtained compound **12**. Secondly, compounds **13a-13m** were prepared according to the procedure reported by our group with some modifications. [21] Compounds **13a-13m** were synthesized from compound **12** reacting with the corresponding acetophenone at room temperature. The mixture of corresponding compounds **3a-3m** and hydrazine hydrate in EtOH was refluxed under stirring for 4 h and the precipitate formed was filtered off, washed with cool ethanol to get compounds **14a-14m**, respectively. Finally, compounds **14a-14m** reacted with the corresponding benzoic acid, together with EDCI and HOBt, respectively. The mixture was refluxed under stirring for 24 h. The corresponding crude product were crystallized with ethanol to give target compounds **15-47**. Compounds **15-47** were fully characterized by ^1H NMR, ESI-MS and elemental analysis.

2.2. Crystal structure of compound **23**

Among these compounds, the crystal structure of compound **23** was determined by X-ray diffraction analysis. The crystal data presented in **Figure 2** and **Table 2** gave perspective views of compound **23** with the atomic labeling system.

2.3. Biological activity

2.3.1. *In Vitro* Antiproliferative Activities.

To test the antiproliferative activities of the synthesized compounds **15-47**, we evaluated the inhibition activities of them against A549 (human lung cancer cell line), MCF-7 (human breast cancer cell line) and HepG-2 (human liver hepatocellular carcinoma cell line). Cells were treated with increasing concentrations of the compounds **15-47**, and viabilities were measured by the MTT assay. The results were summarized in **Table 3**. Among them, Compound **18** displayed the most potent inhibitory activity against three cell lines. Meanwhile, compound **18** could inhibit A549, MCF-7 and HepG-2 at the level of IC_{50} value less than $0.1 \mu\text{M}$. ($\text{IC}_{50} = 0.07 \mu\text{M}$, $0.05 \mu\text{M}$, $0.03 \mu\text{M}$, respectively), comparable to the positive compound CA-4.

Based on the data of **Table 3** obtained, we drew that when $R_2=3, 4, 5$ -trimethyl group, the activity of the tested compounds may be correlated to the variation and modifications of the structure. Obviously, the antiproliferative activities of compounds **15-19** were more potent than compounds **21-27**. In comparison to these target compounds, the inhibitory activity of these compounds with different substituents on the B ring increased in the following order: $4\text{-OCH}_3 > 4\text{-OCH}_2\text{CH}_3 > 4\text{-F} > 4\text{-CH}_3 > 4\text{-H} > 4\text{-Br} > 4\text{-Cl}$; $4\text{-OCH}_3 > 3, 4\text{-diOCH}_3 > 3\text{-OCH}_3 > 2\text{-OCH}_3$; $4\text{-Cl} > 3\text{-Cl}$; $4\text{-CH}_3 > 3\text{-CH}_3$. Then, we drew three conclusions as follows: the para-position substituent is more potent than the meta-position and ortho-position on the B ring; the electron-donating group on the B ring may have improved the antiproliferative activity of the agents; when the substitutions on the B ring are 3, 4, 5-trimethyl, the inhibitory activity is lower. We guessed 3, 4, 5-trimethyl increased the steric.

It was also found that when the substituent on the C ring changed to 4-Br, 4-Cl, the antiproliferative activities of most compounds were lower or totally lost. For example, the antiproliferative activities of compounds **32, 33, 41, 47** are all moderate. Even the IC_{50} values of compounds **28-30, 34, 35, 37-39** are more than $40 \mu\text{M}$. We also drew that when the substituent is 4- OCH_3 on the B ring, the electron-donating group on the C ring may have improved antiproliferative activity of the agents. What was surprising was that compounds **23, 40** and **46** displayed a potent inhibitory activity against A459 MCF-7 and HepG-2. We guessed that the 4-F on the B ring or C ring played a very important role.

2.3.2. Inhibition of tubulin polymerization

To investigate whether the antiproliferative activities of compounds **15-47** derived from an interaction with tubulin or not, these agents were evaluated for their inhibition of tubulin polymerization (**Table 3**). As expected, compound **18** displayed the most potent activity of anti-tubulin polymerization ($IC_{50} = 1.88 \mu\text{M}$) and it suggested that the IC_{50} values of these compounds showed a similar tendency with their relevant IC_{50} values of the antiproliferative assay. However, when comparing the inhibition of tubulin polymerization versus the growth inhibitory effects, we found a positive correlation for most, but not all, of the active compounds.

The next molecular docking of all the synthesized compounds will help us to analyze these results.

2.3.3. Compound 18 induced apoptosis.

To characterize the mode of cell death induced by compound **18**, a biparametric cytofluorimetric analysis was performed using propidium iodide (PI), which stains DNA and enters only dead cells, and fluorescent immunolabeling of the protein annexin-V, which binds to phosphatidyl serine (PS) in a highly selective manner. [22]

HepG-2 cells were treated with compound **18** at 0.01 μM , 0.03 μM and 0.05 μM for 24 h, respectively and DMSO served as the control. The results showed that the percentage of cell apoptosis was 3.89 % at 0 μM for compound **18**, and cell apoptosis was increased to 5.12%, 8.72%, and 13.4% at 0.01 μM , 0.03 μM , and 0.05 μM , respectively (**Figure 3**). Thus, compound **18** could cause cell apoptosis like other tubulin-binding agents.

2.3.4. Analysis of Cell Cycle.

The effect of compound **18** on cell cycle progression was examined by flow cytometry in HepG-2 cells (**Figure 4**). At higher concentration of 0.10 ~ 0.05 μM up to 52.20 % of the cells were arrested in G2/M. There was a concomitant decrease of cells in the other phases of the cell cycle (G1 and S) as shown in **Figure 4**. These findings confirmed a continuing impairment of cell division and proved that compound **8** was a potent antitubulin agent.

2.4. Docking simulations

To gain better understanding on the potency of the synthesized compounds **15-47** and guide further SAR studies, we proceeded to examine the interaction of compounds **15-47** with tubulin crystal structure (PDB code: 1SA0) using the Discovery Studio (version 3.5). We described the CDOCKER_INTERACTION_ENERGY of molecular docking with **Figure 5**. It is clear that compound **18**, shows lowest interaction energy of all the synthesized compounds and the interaction energy reached up to -60.69 kcal/mol.

To take more directly insight into the binding mode of compound **18** and tubulin, we presented the docking results with two pictures (**Figure 6A**, **Figure 6B**) Visual

inspection of the pose of compound **18** into tubulin binding site revealed that compound **18** was tightly embedded into the ATP binding pocket (**Figure 7**). In the binding model, compound **18** is nicely bound to tubulin protein in the ATP-binding site via four hydrogen bonds. The oxygen atom of methoxy on the B ring contributes to the hydrogen bonding interaction (O...H-N: 2.5 Å) with the hydrogen atom on the main chain of LYS 254. The oxygen atom of methoxy on the C ring contributes to the hydrogen bonding interactions (O...H-N: 2.1 Å, O...H-N: 1.9 Å) with the hydrogen atom on the main chain of CYS241. The oxygen atom of the benzo [d] [1, 3] dioxole forms the hydrogen bonding interactions with LYS 352(O...H-N: 2.5 Å).

3. Conclusions

In this study, a series of novel pyrazoline-containing derivatives (compounds **15-47**) have been synthesized and evaluated for their biological activities. Among these small molecules, most of the compounds showed potent *in vitro* inhibitory activity in the tubulin polymerization and cellular assays. Among these small molecules, compound **18** displayed the most potent activity against tubulin assembling, A549, MCF-7 and HepG-2 cell lines ($IC_{50} = 1.88 \mu\text{M}$, $0.07\mu\text{M}$, $0.05\mu\text{M}$, $0.03\mu\text{M}$, respectively), being comparable to the positive compound CA-4. Furthermore, we also showed that compound **18** was a potent inducer of apoptosis in HepG-2 cells and it had cellular effects typical for microtubule interacting agents, causing accumulation of cells in the G2/M phase of the cell cycle. These results, along with molecular docking observations, could provide an important basis for further development of compound **18** as a potent tubulin polymerization inhibitors. Compound **23** and **46** also have attract our attentions. Further studies to improve tubulin polymerization inhibitors and kinases selectivity are now in progress.

4. Experimental.

4.1. Chemistry general

All chemicals and reagents of analytical grade used were purchased from Aldrich (USA). Melting points (uncorrected) were determined on a XT4MP apparatus (Taike Corp, Beijing, China). All the ^1H NMR spectra were recorded on a Bruker DPX 300

model Spectrometer at 25 °C with TMS and solvent signals allotted as internal standards, and chemical shifts were reported in ppm (*d*). ESI-MS spectra were recorded on a Mariner System 5304 Mass spectrometer. Elemental analyses were performed on a CHN-O-Rapid instrument and were within 0.4% of the theoretical values. TLC was performed on the glass-backed silica gel sheets (Silica Gel 60 GF254) and visualized in UV light (254 nm). Column chromatography was performed using silica gel (200-300 mesh) eluting with ethyl acetate and petroleum ether.

4.1.1. Synthesis of 1, 3-benzodioxole-5-carbaldehyde (**12**) [22]

A solution of 3, 4-dihydroxybenzaldehyde (10 g, 0.073 mol, **11**) in DMF (150 mL) was added dropwise to a suspension of CH₂Cl₂ (7 mL, 0.108 mol) and K₂CO₃ (20 g, 0.144 mol) in DMF (300 mL). The mixture was stirred and heated to reflux for 4 h then cooled and filtered. The filtrate was concentrated, diluted with water and extracted with diethyl ether (3100 mL). The filtered cake was washed with diethyl ether (100 mL). The ethereal extracts were combined, washed with 10% NaOH (100 mL), water (100 mL), dried (Na₂SO₄) and evaporated to give 1, 3-benzodioxole-5-carbaldehyde (**12**) a light brown solid. The crude **12** was used in the next step without any further purification.

4.1.2. (E)-3-(benzo[d][1,3]dioxol-5-yl)-1-(4-ethoxyphenyl)prop-2-en-1-one (**13a**) [21]

To a stirred solution of 1-(3-ethoxyphenyl) ethanone (1 mmol) and 1, 3-benzodioxole-5-carbaldehyde (**12**, 1 mmol) in ethanol (30 mL), 6 mol KOH (4 mL) was added and the reaction mixture was stirred until the solids fully formed. The products were filtrated and washed carefully with ice water and cool ethanol, and purified by crystallization from ethanol in refrigerator to give (E)-3-(benzo[d][1,3]dioxol-5-yl)-1-(3-ethoxyphenyl)prop-2-en-1-one (**13a**) a yellow powder, yield 60%. The corresponding acetophenone following this way, we get pure compound **13b-13m** with a yield of 60 - 87%.

4.1.3. 5-(benzo[d][1,3]dioxol-5-yl)-3-(4-ethoxyphenyl)-4,5-dihydro-1H-pyrazole (14a) [21]

To a solution of compound **13a** (1 mmol) in isopropanol (5 mL) hydrazine hydrate (0.2 mL, 4 mmol) was added. The mixture was refluxed under stirring for 4 h, stored at 4 - 5 °C for 1 h, and the precipitate formed was filtered off, washed with cool isopropanol (10 ml), next washed with petroleum ether (10 ml) for three times. We can get white powder, yield 40%. The crude **14a** was used in the next step without any further purification. The compound **13a-13m** following this way, we get crude compound **14b-14m** with a yield of 30-55%.

4.1.4.

(5-(benzo[d][1,3]dioxol-5-yl)-3-(4-ethoxyphenyl)-4,5-dihydro-1H-pyrazol-1-yl)(3, 4, 5-trimethoxyphenyl) methanone (15)

White powders, yield 47.7%. mp: 102 ~ 103 °C. ¹H NMR (DMSO-*d*₆, 300 MHz) δ: 7.71 (s, 1H), 7.68 (s, 1H), 7.32 (s, 2H), 7.03 (s, 1H), 7.01 (s, 1H), 6.87 (t, *J* = 6.00 Hz, 2H), 6.77 (d, *J* = 5.88 Hz, 1H), 5.99 (s, 2H), 5.65 (dd, *J* = 3.48 and 8.61 Hz, 1H), 4.08 (q, *J* = 5.19 Hz, 2H), 3.84 (s, 7H), 3.75 (s, 3H), 3.14 (dd, *J* = 3.63 and 13.50 Hz, 1H), 1.34 (t, *J* = 5.22 Hz, 3H). ¹³C NMR (DMSO-*d*₆, 100 MHz) δ: 164.36, 160.79, 155.58, 125.46, 147.94, 146.81, 140.23, 136.92, 129.85, 128.84, 123.93, 119.35, 115.23, 108.78, 108.07, 106.70, 101.46, 63.79, 61.21, 60.60, 56.43, 55.39, 41.73, 15.00. MS (ESI): 505.53 [M+H]⁺. Anal. calc. for C₂₈H₂₈N₂O₇: C, 66.66; H, 5.59; N, 5.55. Found: C, 66.67; H, 5.58; N, 5.54.

4.1.5.

(5-(benzo[d][1,3]dioxol-5-yl)-3-(2-methoxyphenyl)-4,5-dihydro-1H-pyrazol-1-yl)(3, 4, 5-trimethoxyphenyl) methanone (16)

White powders, yield 46.3%. mp: 178 ~ 179 °C. ¹H NMR (DMSO-*d*₆, 300 MHz) δ: 7.79 ~ 7.81 (m, 1H), 7.42 ~ 7.47 (m, 1H), 7.33 (s, 2H), 7.13 (d, *J* = 6.21 Hz, 1H), 7.03 (t, *J* = 5.76 Hz, 1H), 6.87 (t, *J* = 6.00 Hz, 2H), 6.78 (d, *J* = 5.94 Hz, 1H), 5.99 (s, 2H), 5.62 (dd, *J* = 3.51 and 8.67 Hz, 1H), 3.92 (dd, *J* = 9.39 and 13.95 Hz, 1H), 3.82 (s, 6H), 3.81 (s, 3H), 3.74 (s, 3H), 3.18 (dd, *J* = 3.63 and 13.98 Hz, 1H). ¹³C NMR

(DMSO- d_6 , 100 MHz) δ : 164.57, 158.62, 154.98, 152.46, 147.96, 146.81, 140.32, 137.04, 132.34, 129.84, 129.04, 129.04, 121.23, 120.39, 119.28, 113.02, 108.80, 108.20, 106.62, 101.46, 61.14, 60.59, 56.46, 56.20, 45.01. MS (ESI): 491.50 [M+H]⁺. Anal. calc. for C₂₇H₂₆N₂O₇: C, 66.11; H, 5.34; N, 5.71. Found: C, 66.12; H, 5.33; N, 5.70.

4.1.6

(5-(benzo[*d*][1,3]dioxol-5-yl)-3-(3-methoxyphenyl)-4,5-dihydro-1*H*-pyrazol-1-yl)(3, 4, 5-trimethoxyphenyl) methanone (17)

White powders, yield 40.6%. mp: 156 ~ 157 °C. ¹H NMR (DMSO- d_6 , 300 MHz) δ : 7.36 ~ 7.42 (m, 4H), 7.29 (s, 1H), 7.06 (d, $J = 5.97$ Hz, 1H), 6.87 (d, $J = 6.00$ Hz, 2H), 6.78 (d, $J = 5.91$ Hz, 1H), 5.99 (s, 2H), 5.68 (dd, $J = 3.60$ and 8.73 Hz, 1H), 3.84 (s, 7H), 3.79 (s, 3H), 3.75 (s, 3H), 3.19 (dd, $J = 3.72$ and 13.62 Hz, 1H). MS (ESI): 491.50 [M+H]⁺. Anal. calc. for C₂₇H₂₆N₂O₇: C, 66.11; H, 5.34; N, 5.71. Found: C, 66.12; H, 5.33; N, 5.70.

4.1.7

(5-(benzo[*d*][1,3]dioxol-5-yl)-3-(4-methoxyphenyl)-4,5-dihydro-1*H*-pyrazol-1-yl)(3, 4, 5-trimethoxyphenyl) methanone (18)

White powders, yield 50.6%. mp: 107 ~ 108 °C. ¹H NMR (DMSO- d_6 , 300 MHz) δ : 7.72 (s, 1H), 7.70 (s, 1H), 7.33 (s, 2H), 7.05 (s, 1H), 7.02 (s, 1H), 6.86 (t, $J = 5.97$ Hz, 2H), 6.77 (d, $J = 5.88$ Hz, 1H), 5.99 (s, 2H), 5.65 (dd, $J = 3.45$ and 8.61 Hz, 1H), 3.83 (s, 7H), 3.80 (s, 3H), 3.75 (s, 3H), 3.14 (dd, $J = 3.60$ and 13.50 Hz, 1H). MS (ESI): 491.50 [M+H]⁺. Anal. calc. for C₂₇H₂₆N₂O₇: C, 66.11; H, 5.34; N, 5.71. Found: C, 66.10; H, 5.33; N, 5.70.

4.1.8

(5-(benzo[*d*][1,3]dioxol-5-yl)-3-(3,4-dimethoxyphenyl)-4,5-dihydro-1*H*-pyrazol-1-yl)(3, 4, 5-trimethoxyphenyl) methanone (19)

White powders, yield 51.5%. mp: 115 ~ 116 °C. ¹H NMR (DMSO- d_6 , 300 MHz) δ : 7.40 (s, 2H), 7.34 (d, $J = 1.32$ Hz, 1H), 7.29 (dd, $J = 1.38$ and 6.24 Hz, 1H), 7.04 (d, $J = 6.36$ Hz, 1H), 6.88 (d, $J = 6.00$ Hz, 1H), 6.83 (s, 1H), 6.76 (d, $J = 5.91$ Hz, 1H), 5.99 (s, 2H), 5.67 (dd, $J = 3.33$ and 8.61 Hz, 1H), 3.85 (s, 7H), 3.80 (s, 3H), 3.78 (s,

3H), 3.75 (s, 3H), 3.17 (dd, $J = 3.48$ and 13.50 Hz, 1H). ^{13}C NMR (DMSO- d_6 , 100 MHz) δ : 164.00, 155.91, 152.48, 151.43, 149.27, 147.95, 147.95, 146.81, 140.35, 138.99, 129.57, 124.13, 121.13, 119.28, 111.99, 109.36, 108.78, 108.25, 106.63, 101.46, 61.32, 60.61, 56.40, 56.09, 56.09, 55.79, 55.38, 41.66. MS (ESI): 521.53 [M+H] $^+$. Anal. calc. for $\text{C}_{28}\text{H}_{28}\text{N}_2\text{O}_8$: C, 64.61; H, 5.42; N, 5.38. Found: C, 64.60; H, 5.43; N, 5.37.

4.1.9.

(5-(benzo[*d*][1,3]dioxol-5-yl)-3-(3,4,5-trimethoxyphenyl)-4,5-dihydro-1*H*-pyrazol-1-yl)(3, 4, 5-trimethoxyphenyl) methanone (20)

White powders, yield 51.2%. mp: 206 ~ 207 °C. ^1H NMR (DMSO- d_6 , 300 MHz) δ : 7.42 (s, 2H), 7.06 (s, 2H), 6.89 (d, $J = 5.97$ Hz, 1H), 6.84 (s, 1H), 6.77 (d, $J = 5.97$ Hz, 1H), 6.00 (s, 2H), 5.72 (dd, $J = 3.36$ and 8.67 Hz, 1H), 3.85 (s, 7H), 3.82 (s, 6H), 3.75 (s, 3H), 3.71 (s, 3H), 3.26 (dd, $J = 3.48$ and 13.62 Hz, 1H). ^{13}C NMR (DMSO- d_6 , 100 MHz) δ : 164.00, 156.01, 153.52, 152.50, 147.97, 146.83, 140.46, 140.03, 136.93, 129.37, 127.02, 119.24, 108.80, 108.29, 106.58, 104.60, 101.48, 61.51, 60.63, 56.41, 56.35, 41.67. MS (ESI): 551.56 [M+H] $^+$. Anal. calc. for $\text{C}_{29}\text{H}_{30}\text{N}_2\text{O}_9$: C, 63.27; H, 5.49; N, 5.09. Found: C, 63.26; H, 5.48; N, 5.08.

4.1.10.

(5-(benzo[*d*][1,3]dioxol-5-yl)-3-(4-bromophenyl)-4,5-dihydro-1*H*-pyrazol-1-yl)(3, 4, 5-trimethoxyphenyl) methanone (21)

White powders, yield 49.5%. mp: 107 ~ 108 °C. ^1H NMR (DMSO- d_6 , 300 MHz) δ : 7.70 (s, 4H), 7.29 (s, 2H), 6.88 (d, $J = 5.88$ Hz, 2H), 6.79 (d, $J = 6.03$ Hz, 1H), 6.00 (s, 2H), 5.69 (dd, $J = 3.78$ and 8.73 Hz, 1H), 3.84 (s, 7H), 3.75 (s, 3H), 3.18 (dd, $J = 3.87$ and 13.62 Hz, 1H). MS (ESI): 540.37 [M+H] $^+$. Anal. calc. for $\text{C}_{26}\text{H}_{23}\text{BrN}_2\text{O}_6$: C, 57.90; H, 4.30; N, 5.19. Found: C, 57.91; H, 4.31; N, 5.18.

4.1.11

(5-(benzo[*d*][1,3]dioxol-5-yl)-3-(4-chlorophenyl)-4,5-dihydro-1*H*-pyrazol-1-yl)(3, 4, 5-trimethoxyphenyl) methanone (22)

White powders, yield 53.5%. mp: 151 ~ 152 °C. ¹H NMR (DMSO-*d*₆, 300 MHz) δ: 7.78 (s, 1H), 7.76 (s, 1H), 7.56 (s, 1H), 7.54 (s, 1H), 7.29 (s, 2H), 6.89 (s, 1H), 6.87 (s, 1H), 6.80 (d, *J* = 6.03 Hz, 1H), 6.00 (s, 2H), 5.69 (dd, *J* = 3.78 and 8.76 Hz, 1H), 3.84 (s, 7H), 3.76 (s, 3H), 3.18 (dd, *J* = 3.84 and 13.59 Hz, 1H). MS (ESI): 495.92 [M+H]⁺. Anal. calc. for C₂₆H₂₃ClN₂O₆: C, 63.10; H, 4.68; N, 5.66. Found: C, 63.11; H, 4.69; N, 5.65.

4.1.12.

(5-(benzo[*d*][1,3]dioxol-5-yl)-3-(4-fluorophenyl)-4,5-dihydro-1*H*-pyrazol-1-yl)(3,4,5-trimethoxyphenyl) methanone (23)

White powders, yield 45.9%. mp: 168 ~ 169 °C. ¹H NMR (DMSO-*d*₆, 300 MHz) δ: 7.82 (q, *J* = 4.14 Hz, 2H), 7.35 (s, 1H), 7.33 (s, 1H), 7.30 (d, *J* = 4.50 Hz, 2H), 6.88 (d, *J* = 6.00 Hz, 2H), 6.79 (d, *J* = 5.97 Hz, 1H), 5.99 (s, 2H), 5.68 (dd, *J* = 3.69 and 8.73 Hz, 1H), 3.83 (s, 7H), 3.75 (s, 3H), 3.18 (dd, *J* = 3.78 and 17.34 Hz, 1H). MS (ESI): 479.47 [M+H]⁺. Anal. calc. for C₂₆H₂₃FN₂O₆: C, 65.27; H, 4.85; N, 5.85. Found: C, 65.26; H, 4.84; N, 5.86.

4.1.13.

(5-(benzo[*d*][1,3]dioxol-5-yl)-3-(3-chlorophenyl)-4,5-dihydro-1*H*-pyrazol-1-yl)(3,4,5-trimethoxyphenyl) methanone (24)

White powders, yield 42.6%. mp: 169 ~ 170 °C. ¹H NMR (DMSO-*d*₆, 300 MHz) δ: 7.95 (s, 1H), 7.75 (d, *J* = 5.85 Hz, 1H), 7.68 (d, *J* = 6.54 Hz, 1H), 7.45 (t, *J* = 5.94 Hz, 1H), 7.33 (s, 2H), 6.88 (t, *J* = 2.25 Hz, 2H), 6.79 (d, *J* = 6.06 Hz, 1H), 6.00 (s, 2H), 5.69 (dd, *J* = 3.66 and 8.76 Hz, 1H), 3.85 (s, 7H), 3.75 (s, 3H), 3.20 (dd, *J* = 3.81 and 13.71 Hz, 1H). MS (ESI): 495.92 [M+H]⁺. Anal. calc. for C₂₆H₂₃ClN₂O₆: C, 63.10; H, 4.68; N, 5.66. Found: C, 63.09; H, 4.67; N, 5.67.

4.1.14.

(5-(benzo[*d*][1,3]dioxol-5-yl)-3-(*p*-tolyl)-4,5-dihydro-1*H*-pyrazol-1-yl)(3,4,5-trimethoxyphenyl) methanone (25)

White powders, yield 42.6%. mp: 145 ~ 146 °C. ¹H NMR (DMSO-*d*₆, 300 MHz) δ: 7.67 (s, 1H), 7.65 (s, 1H), 7.33 (s, 2H), 7.29 (s, 1H), 7.27 (s, 1H), 6.86 (t, *J* = 6.00 Hz, 2H), 6.78 (d, *J* = 5.94 Hz, 1H), 5.99 (s, 2H), 5.66 (dd, *J* = 3.57 and 8.64 Hz, 1H), 3.83

(s, 7H), 3.75 (s, 3H), 3.15 (dd, $J = 3.69$ and 13.56 Hz, 1H), 2.34 (s, 3H). MS (ESI): 475.51 [M+H]⁺. Anal. calc. for C₂₇H₂₆N₂O₆: C, 68.34; H, 5.52; N, 5.90. Found: C, 68.33; H, 5.51; N, 5.91.

4.1.15.

(5-(benzo[*d*][1,3]dioxol-5-yl)-3-(*m*-tolyl)-4,5-dihydro-1*H*-pyrazol-1-yl)(3,4,5-trimethoxyphenyl) methanone (26)

White powders, yield 49.6%. mp: 159 ~ 160 °C. ¹H NMR (DMSO-*d*₆, 300 MHz) δ: 7.61 (s, 1H), 7.56 (d, $J = 5.76$ Hz, 1H), 7.35 ~ 7.38 (m, 3H), 7.29 (d, $J = 5.67$ Hz, 1H), 6.87 (t, $J = 6.00$ Hz, 2H), 6.77 (d, $J = 5.88$ Hz, 1H), 5.99 (s, 2H), 5.68 (dd, $J = 3.48$ and 8.67 Hz, 1H), 3.85 (s, 7H), 3.75 (s, 3H), 3.16 (dd, $J = 3.60$ and 13.56 Hz, 1H), 2.34 (s, 3H). MS (ESI): 475.51 [M+H]⁺. Anal. calc. for C₂₇H₂₆N₂O₆: C, 68.34; H, 5.52; N, 5.90. Found: C, 68.35; H, 5.51; N, 5.91.

4.1.16.

(5-(benzo[*d*][1,3]dioxol-5-yl)-3-phenyl-4,5-dihydro-1*H*-pyrazol-1-yl)(3,4,5-trimethoxyphenyl) methanone (27)

White powders, yield 37.6%. mp: 149 ~ 150 °C. ¹H NMR (DMSO-*d*₆, 300 MHz) δ: 7.76 ~ 7.78 (m, 2H), 7.48 (d, $J = 4.80$ Hz, 3H), 7.32 (s, 2H), 6.88 (d, $J = 6.06$ Hz, 2H), 6.79 (d, $J = 6.03$ Hz, 1H), 5.99 (s, 2H), 5.68 (dd, $J = 3.63$ and 8.67 Hz, 1H), 3.84 (s, 7H), 3.75 (s, 3H), 3.18 (dd, $J = 3.75$ and 13.59 Hz, 1H). MS (ESI): 461.48 [M+H]⁺. Anal. calc. for C₂₆H₂₄N₂O₆: C, 67.82; H, 5.25; N, 6.08. Found: C, 67.81; H, 5.24; N, 6.07.

4.1.17.

(5-(benzo[*d*][1,3]dioxol-5-yl)-3-(4-ethoxyphenyl)-4,5-dihydro-1*H*-pyrazol-1-yl)(4-bromophenyl) methanone (28)

White powders, yield 57.3%. mp: 147 ~ 148 °C. ¹H NMR (DMSO-*d*₆, 300 MHz) δ: 7.84 (s, 1H), 7.82 (s, 1H), 7.71 (s, 1H), 7.69 (s, 1H), 7.66 (s, 1H), 7.64 (s, 1H), 7.00 (s, 1H), 6.98 (s, 1H), 6.87 (t, $J = 6.00$ Hz, 2H), 6.78 (d, $J = 5.97$ Hz, 1H), 6.00 (s, 2H), 5.66 (dd, $J = 3.54$ and 8.64 Hz, 1H), 4.06 (q, $J = 5.19$ Hz, 2H), 3.83 (dd, $J = 8.76$ and 13.53 Hz, 1H), 3.15 (dd, $J = 3.66$ and 13.53 Hz, 1H), 1.33 (t, $J = 5.19$ Hz, 3H). MS (ESI): 494.35 [M+H]⁺. Anal. calc. for C₂₅H₂₁BrN₂O₄: C, 60.86; H, 4.29; N, 5.68.

Found: C, 60.89; H, 4.28; N, 5.67.

4.1.18.

(5-(benzo[*d*][1,3]dioxol-5-yl)-3-(2-methoxyphenyl)-4,5-dihydro-1*H*-pyrazol-1-yl)(4-bromophenyl) methanone (29)

White powders, yield 43.2%. mp: 148 ~ 149 °C. ¹H NMR (DMSO-*d*₆, 300 MHz) δ: 7.88 (s, 1H), 7.85 (s, 1H), 7.67 ~ 7.72 (m, 3H), 7.42 ~ 7.46 (m, 1H), 7.11 (d, *J* = 6.18 Hz, 1H), 7.00 (t, *J* = 5.76 Hz, 1H), 6.86 (t, *J* = 5.97 Hz, 2H), 6.76 (d, *J* = 5.97 Hz, 1H), 5.99 (s, 2H), 5.63 (dd, *J* = 3.51 and 8.67 Hz, 1H), 3.91 (dd, *J* = 8.79 and 13.95 Hz, 1H), 3.82 (s, 3H), 3.19 (dd, *J* = 3.60 and 13.95 Hz, 1H). ¹³C NMR (DMSO-*d*₆, 100 MHz) δ: 164.60, 158.59, 155.38, 148.02, 146.89, 136.76, 134.18, 132.39, 132.15, 131.25, 129.41, 124.94, 121.13, 120.18, 119.28, 112.85, 108.83, 106.54, 101.49, 60.66, 56.23, 45.17. MS (ESI): 480.32 [M+H]⁺. Anal. calc. for C₂₄H₁₉BrN₂O₄: C, 60.14; H, 4.00; N, 5.84. Found: C, 60.15; H, 4.01; N, 5.85.

4.1.19.

(5-(benzo[*d*][1,3]dioxol-5-yl)-3-(3-methoxyphenyl)-4,5-dihydro-1*H*-pyrazol-1-yl)(4-bromophenyl) methanone (30)

White powders, yield 56.3%. mp: 159 ~ 160 °C. ¹H NMR (DMSO-*d*₆, 300 MHz) δ: 7.86 (s, 1H), 7.84 (s, 1H), 7.72 (s, 1H), 7.70 (s, 1H), 7.32 ~ 7.41 (m, 2H), 7.24 (s, 1H), 7.06 (d, *J* = 6.00 Hz, 1H), 6.90 (s, 1H), 6.87 (d, *J* = 2.70 Hz, 1H), 6.80 (d, *J* = 5.91 Hz, 1H), 6.00 (s, 2H), 5.70 (dd, *J* = 3.63 and 8.70 Hz, 1H), 3.88 (dd, *J* = 8.85 and 13.65 Hz, 1H), 3.80 (s, 3H), 3.22 (dd, *J* = 3.75 and 13.65 Hz, 1H). MS (ESI): 480.32 [M+H]⁺. Anal. calc. for C₂₄H₁₉BrN₂O₄: C, 60.14; H, 4.00; N, 5.84. Found: C, 60.15; H, 5.83; N, 5.85.

4.1.20.

(5-(benzo[*d*][1,3]dioxol-5-yl)-3-(4-methoxyphenyl)-4,5-dihydro-1*H*-pyrazol-1-yl)(4-bromophenyl) methanone (31)

White powders, yield 40.2%. mp: 175 ~ 176 °C. ¹H NMR (DMSO-*d*₆, 300 MHz) δ: 7.85 (s, 1H), 7.83 (s, 1H), 7.69 (t, *J* = 6.42 Hz, 4H), 7.02 (s, 1H), 7.00 (s, 1H), 6.87 (t, *J* = 5.97 Hz, 2H), 6.79 (d, *J* = 5.91 Hz, 1H), 6.00 (s, 2H), 5.66 (dd, *J* = 3.54 and 8.64 Hz, 1H), 3.80 (s, 4H), 3.16 (dd, *J* = 3.66 and 13.53 Hz, 1H). MS (ESI): 480.32 [M+H]⁺

⁺. Anal. calc. for C₂₄H₁₉BrN₂O₄: C, 60.14; H, 4.00; N, 5.84. Found: C, 60.13; H, 4.01; N, 5.85.

4.1.21.

(5-(benzo[*d*][1,3]dioxol-5-yl)-3-(3,4-dimethoxyphenyl)-4,5-dihydro-1*H*-pyrazol-1-yl)(4-bromophenyl) methanone (32)

White powders, yield 39.5%. mp: 181 ~ 182 °C. ¹H NMR (DMSO-*d*₆, 300 MHz) δ: 7.88 (d, *J* = 6.21 Hz, 2H), 7.72 (s, 1H), 7.70 (s, 1H), 7.30 (s, 1H), 7.28 (s, 1H), 7.03 (d, *J* = 6.57 Hz, 1H), 6.88 (t, *J* = 6.00 Hz, 2H), 6.78 (d, *J* = 5.97 Hz, 1H), 6.00 (s, 2H), 5.68 (dd, *J* = 3.42 and 8.61 Hz, 1H), 3.81 (s, 4H), 3.79 (s, 3H), 3.20 (dd, *J* = 3.54 and 13.53 Hz, 1H). MS (ESI): 510.35 [M+H]⁺. Anal. calc. for C₂₅H₂₁BrN₂O₅: C, 58.95; H, 4.16; N, 5.50. Found: C, 58.94; H, 4.15; N, 5.51.

4.1.22.

(5-(benzo[*d*][1,3]dioxol-5-yl)-3-(3,4,5-trimethoxyphenyl)-4,5-dihydro-1*H*-pyrazol-1-yl)(4-bromophenyl) methanone (33)

White powders, yield 51.6%. mp: 190 ~ 191 °C. ¹H NMR (DMSO-*d*₆, 300 MHz) δ: 7.90 (d, *J* = 6.18 Hz, 2H), 7.72 (s, 1H), 7.70 (s, 1H), 7.03 (s, 2H), 6.88 (t, *J* = 6.00 Hz, 2H), 6.78 (d, *J* = 5.88 Hz, 1H), 6.00 (s, 2H), 5.71 (dd, *J* = 3.39 and 8.64 Hz, 1H), 3.82 (s, 7H), 3.71 (s, 3H), 3.28 (dd, *J* = 3.54 and 13.62 Hz, 1H). ¹³C NMR (DMSO-*d*₆, 100 MHz) δ: 164.36, 155.31, 153.47, 148.05, 146.93, 140.13, 136.60, 133.95, 132.29, 131.26, 126.82, 125.12, 119.28, 108.81, 106.54, 104.83, 101.51, 61.14, 60.62, 56.45, 42.07. MS (ESI): 540.37 [M+H]⁺. Anal. calc. for C₂₆H₂₃BrN₂O₆: C, 57.90; H, 4.30; N, 5.19. Found: C, 57.91; H, 4.31; N, 5.18.

4.1.23.

(5-(benzo[*d*][1,3]dioxol-5-yl)-3-(4-bromophenyl)-4,5-dihydro-1*H*-pyrazol-1-yl)(4-bromophenyl) methanone (34)

White powders, yield 45.7%. mp: 186 ~ 187 °C. ¹H NMR (DMSO-*d*₆, 300 MHz) δ: 7.82 (s, 1H), 7.80 (s, 1H), 7.70 (s, 1H), 7.68 (s, 1H), 7.65 (s, 4H), 6.87 (t, *J* = 6.00 Hz, 2H), 6.79 (d, *J* = 6.12 Hz, 1H), 6.00 (s, 2H), 5.68 (dd, *J* = 3.78 and 8.73 Hz, 1H), 3.86 (dd, *J* = 8.88 and 13.65 Hz, 1H), 3.18 (dd, *J* = 3.90 and 13.68 Hz, 1H). ¹³C NMR (DMSO-*d*₆, 100 MHz) δ: 164.97, 155.29, 148.05, 146.98, 136.40, 134.10, 132.26,

132.01, 131.34, 130.64, 129.24, 125.01, 124.38, 119.54, 108.79, 106.71, 101.51, 61.12, 41.89. MS (ESI): 529.19 [M+H]⁺. Anal. calc. for C₂₃H₁₆Br₂N₂O₃: C, 52.30; H, 3.05; N, 5.30. Found: C, 52.31; H, 3.04; N, 5.31.

4.1.24.

(5-(benzo[*d*][1,3]dioxol-5-yl)-3-(4-chlorophenyl)-4,5-dihydro-1*H*-pyrazol-1-yl)(4-bromophenyl) methanone (35)

White powders, yield 50.5%. mp: 173 ~ 174 °C. ¹H NMR (DMSO-*d*₆, 300 MHz) δ: 7.82 (d, *J* = 5.79 Hz, 2H), 7.71 (dd, *J* = 10.17 Hz, 4H), 7.52 (d, *J* = 6.06 Hz, 2H), 6.84 (d, *J* = 18.21 Hz, 3H), 5.99 (s, 2H), 5.69 (dd, *J* = 3.30 and 8.43 Hz, 1H), 3.87 (dd, *J* = 9.03 and 13.53 Hz, 1H), 3.19 (dd, *J* = 3.93 and 13.59 Hz, 1H). MS (ESI): 484.74 [M+H]⁺. Anal. calc. for C₂₃H₁₆BrClN₂O₃: C, 57.11; H, 3.33; N, 5.79. Found: C, 57.10; H, 3.34; N, 5.78.

4.1.25.

(5-(benzo[*d*][1,3]dioxol-5-yl)-3-(4-fluorophenyl)-4,5-dihydro-1*H*-pyrazol-1-yl)(4-bromophenyl) methanone (36)

White powders, yield 52.5%. mp: 153 ~ 154 °C. ¹H NMR (DMSO-*d*₆, 300 MHz) δ: 7.76 ~ 7.84 (m, 4H), 7.71 (s, 1H), 7.69 (s, 1H), 7.30 (t, *J* = 6.63 Hz, 2H), 6.88 (d, *J* = 5.85 Hz, 2H), 6.80 (d, *J* = 6.03 Hz, 1H), 5.99 (s, 2H), 5.68 (dd, *J* = 3.69 and 8.70 Hz, 1H), 3.89 (dd, *J* = 8.82 and 13.62 Hz, 1H), 3.20 (dd, *J* = 3.81 and 13.65 Hz, 1H). MS (ESI): 468.29 [M+H]⁺. Anal. calc. for C₂₃H₁₆BrFN₂O₃: C, 59.12; H, 3.45; N, 5.99. Found: C, 59.11; H, 3.46; N, 6.00.

4.1.26.

(5-(benzo[*d*][1,3]dioxol-5-yl)-3-(*p*-tolyl)-4,5-dihydro-1*H*-pyrazol-1-yl)(4-bromophenyl) methanone (37)

White powders, yield 55.7%. mp: 159 ~ 160 °C. ¹H NMR (DMSO-*d*₆, 300 MHz) δ: 7.84 (s, 1H), 7.82 (s, 1H), 7.71 (s, 1H), 7.69 (s, 1H), 7.63 (s, 1H), 7.61 (s, 1H), 7.27 (s, 1H), 7.25 (s, 1H), 6.87 (t, *J* = 6.00 Hz, 2H), 6.78 (d, *J* = 5.94 Hz, 1H), 5.99 (s, 2H), 5.67 (dd, *J* = 3.60 and 8.64 Hz, 1H), 3.85 (dd, *J* = 8.82 and 13.59 Hz, 1H), 3.16 (dd, *J* = 3.75 and 13.59 Hz, 1H), 2.34 (s, 3H). MS (ESI): 464.32 [M+H]⁺. Anal. calc. for C₂₄H₁₉BrN₂O₃: C, 62.22; H, 4.13; N, 6.05. Found: C, 62.21; H, 4.14; N, 6.06.

4.1.27.**(5-(benzo[*d*][1,3]dioxol-5-yl)-3-(*m*-tolyl)-4,5-dihydro-1*H*-pyrazol-1-yl)(4-bromophenyl) methanone (38)**

White powders, yield 47.7%. mp: 155 ~ 156 °C. ¹H NMR (DMSO-*d*₆, 300 MHz) δ: 7.85 (s, 1H), 7.82 (s, 1H), 7.71 (s, 1H), 7.69 (s, 1H), 7.54 (s, 2H), 7.34 (t, *J* = 5.76 Hz, 1H), 7.28 (d, *J* = 5.70 Hz, 1H), 6.87 (t, *J* = 6.00 Hz, 2H), 6.79 (d, *J* = 5.94 Hz, 1H), 5.99 (s, 2H), 5.68 (dd, *J* = 3.57 and 8.67 Hz, 1H), 3.86 (dd, *J* = 8.82 and 13.59 Hz, 1H), 3.18 (dd, *J* = 3.66 and 13.59 Hz, 1H), 2.33 (s, 3H). MS (ESI): 464.32 [M+H]⁺. Anal. calc. for C₂₄H₁₉BrN₂O₃: C, 62.22; H, 4.13; N, 6.05. Found: C, 62.21; H, 4.14; N, 6.04.

4.1.28.**(5-(benzo[*d*][1,3]dioxol-5-yl)-3-phenyl-4,5-dihydro-1*H*-pyrazol-1-yl)(4-bromophenyl) methanone (39)**

White powders, yield 48.1%. mp: 144 ~ 145 °C. ¹H NMR (DMSO-*d*₆, 300 MHz) δ: 7.85 (s, 1H), 7.83 (s, 1H), 7.72 (t, *J* = 6.27 Hz, 4H), 7.46 (d, *J* = 5.22 Hz, 3H), 6.88 (t, *J* = 6.00 Hz, 2H), 6.80 (d, *J* = 6.03 Hz, 1H), 6.00 (s, 2H), 5.69 (dd, *J* = 3.69 and 8.73 Hz, 1H), 3.88 (dd, *J* = 8.82 and 13.62 Hz, 1H), 3.20 (dd, *J* = 3.75 and 13.59 Hz, 1H). MS (ESI): 450.30 [M+H]⁺. Anal. calc. for C₂₃H₁₇BrN₂O₃: C, 61.48; H, 3.81; N, 6.23. Found: C, 61.47; H, 3.82; N, 6.24.

4.1.29.**(5-(benzo[*d*][1,3]dioxol-5-yl)-3-(4-methoxyphenyl)-4,5-dihydro-1*H*-pyrazol-1-yl)(4-fluorophenyl) methanone (40)**

White powders, yield 42.6%. mp: 154 ~ 155 °C. ¹H NMR (DMSO-*d*₆, 300 MHz) δ: 7.99 (t, *J* = 5.85 Hz, 2H), 7.69 (s, 1H), 7.67 (s, 1H), 7.32 (t, *J* = 6.63 Hz, 2H), 7.03 (s, 1H), 7.01 (s, 1H), 6.87 (t, *J* = 5.97 Hz, 2H), 6.79 (d, *J* = 5.94 Hz, 1H), 5.99 (s, 2H), 5.67 (dd, *J* = 3.54 and 8.64 Hz, 1H), 3.84 (dd, *J* = 8.79 and 13.53 Hz, 1H), 3.80 (s, 3H), 3.15 (dd, *J* = 3.66 and 13.53 Hz, 1H). MS (ESI): 419.42 [M+H]⁺. Anal. calc. for C₂₄H₁₉FN₂O₄: C, 68.89; H, 4.58; N, 6.70. Found: C, 68.88; H, 4.59; N, 6.69.

4.1.30.

(5-(benzo[*d*][1,3]dioxol-5-yl)-3-(4-methoxyphenyl)-4,5-dihydro-1*H*-pyrazol-1-yl)(4-chlorophenyl) methanone (41)

White powders, yield 48.6%. mp: 140 ~ 141 °C. ¹H NMR (DMSO-*d*₆, 300 MHz) δ: 7.93 (s, 1H), 7.91 (s, 1H), 7.69 (s, 1H), 7.67 (s, 1H), 7.57 (s, 1H), 7.55 (s, 1H), 7.02 (s, 1H), 7.00 (s, 1H), 7.87 (t, *J* = 6.00 Hz, 2H), 6.79 (d, *J* = 5.91 Hz, 1H), 6.00 (s, 2H), 5.67 (dd, *J* = *J* = 3.56 and 8.68 Hz, 1H), 3.84 (dd, *J* = 8.75 and 13.50 Hz, 1H), 3.80 (s, 3H), 3.16 (dd, *J* = 3.66 and 13.59 Hz, 1H). MS (ESI): 435.87 [M+H]⁺. Anal. calc. for C₂₄H₁₉ClN₂O₄: C, 66.29; H, 4.40; N, 6.44. Found: C, 66.28; H, 4.41; N, 6.43.

4.1.31.

(5-(benzo[*d*][1,3]dioxol-5-yl)-3-(4-methoxyphenyl)-4,5-dihydro-1*H*-pyrazol-1-yl)(3-methoxyphenyl) methanone (42)

White powders, yield 35.9%. mp: 166 ~ 167 °C. ¹H NMR (DMSO-*d*₆, 300 MHz) δ: 7.85 (s, 1H), 7.83 (s, 1H), 7.65 (s, 1H), 7.62 (s, 1H), 7.47 ~ 7.54 (m, 2H), 7.03 (s, 1H), 7.00 (s, 1H), 6.88 (t, *J* = 6.00 Hz, 2H), 6.79 (d, *J* = 5.97 Hz, 1H), 6.00 (s, 2H), 5.68 (dd, *J* = 3.50 and 8.66 Hz, 1H), 3.84 (s, 4H), 3.80 (s, 3H), 3.19 (dd, *J* = 3.66 and 13.59 Hz, 1H). MS (ESI): 431.45 [M+H]⁺. Anal. calc. for C₂₅H₂₂N₂O₅: C, 69.76; H, 5.15; N, 6.51. Found: C, 69.77; H, 5.14; N, 6.50.

4.1.32.

(5-(benzo[*d*][1,3]dioxol-5-yl)-3-(4-methoxyphenyl)-4,5-dihydro-1*H*-pyrazol-1-yl)(4-methoxyphenyl) methanone (43)

White powders, yield 31.2%. mp: 146 ~ 147 °C. ¹H NMR (DMSO-*d*₆, 300 MHz) δ: 7.97 (t, *J* = 5.81 Hz, 2H), 7.66 (s, 1H), 7.64 (s, 1H), 7.32 (t, *J* = 6.60 Hz, 2H), 7.03 (s, 1H), 7.00 (s, 1H), 6.87 (t, *J* = 5.97 Hz, 2H), 6.79 (d, *J* = 5.94 Hz, 1H), 5.99 (s, 2H), 5.68 (dd, *J* = 3.50 and 8.66 Hz, 1H), 3.84 (s, 4H), 3.80 (s, 3H), 3.19 (dd, *J* = 3.66 and 13.59 Hz, 1H). MS (ESI): 431.45 [M+H]⁺. Anal. calc. for C₂₅H₂₂N₂O₅: C, 69.76; H, 5.15; N, 6.51. Found: C, 69.78; H, 5.14; N, 6.50.

4.1.33.

(5-(benzo[*d*][1,3]dioxol-5-yl)-3-(4-methoxyphenyl)-4,5-dihydro-1*H*-pyrazol-1-yl)(3,4-dimethoxyphenyl) methanone (44)

White powders, yield 44.6%. mp: 150 ~ 151 °C. ¹H NMR (DMSO-*d*₆, 300 MHz) δ : 7.80 (s, 1H), 7.78 (s, 1H), 7.62 (s, 1H), 7.60 (s, 1H), 7.47 ~ 7.54 (m, 1H), 7.01 (s, 1H), 7.00 (s, 1H), 6.87 (t, *J* = 6.00 Hz, 2H), 6.78 (d, *J* = 5.97 Hz, 1H), 6.00 (s, 2H), 5.68 (dd, *J* = 3.50 and 8.66 Hz, 1H), 3.84 (s, 4H), 3.82 (s, 3H), 3.80 (s, 3H), 3.18 (dd, *J* = 3.66 and 13.59 Hz, 1H). MS (ESI): 461.48 [M+H]⁺. Anal. calc. for C₂₆H₂₄N₂O₆: C, 67.82; H, 5.25; N, 6.08. Found: C, 67.81; H, 5.24; N, 6.09.

4.1.34.

(5-(benzo[*d*][1,3]dioxol-5-yl)-3-(4-methoxyphenyl)-4,5-dihydro-1*H*-pyrazol-1-yl)(phenyl) methanone (45)

White powders, yield 41.9%. mp: 152 ~ 153 °C. ¹H NMR (DMSO-*d*₆, 300 MHz) δ : 7.89 (s, 1H), 7.87 (s, 1H), 7.67 (s, 1H), 7.65 (s, 1H), 7.47 ~ 7.54 (m, 3H), 7.03 (s, 1H), 7.00 (s, 1H), 6.88 (t, *J* = 6.00 Hz, 2H), 6.79 (d, *J* = 5.97 Hz, 1H), 6.00 (s, 2H), 5.68 (dd, *J* = 3.51 and 8.67 Hz, 1H), 3.84 (dd, *J* = 8.76 and 13.50 Hz, 1H), 3.80 (s, 3H), 3.19 (dd, *J* = 3.63 and 13.50 Hz, 1H). MS (ESI): 401.43 [M+H]⁺. Anal. calc. for C₂₄H₂₀N₂O₄: C, 71.99; H, 5.03; N, 7.00. Found: C, 71.98; H, 5.04; N, 7.01.

4.1.35.

(5-(benzo[*d*][1,3]dioxol-5-yl)-3-(3,4,5-trimethoxyphenyl)-4,5-dihydro-1*H*-pyrazol-1-yl)(4-fluorophenyl)methanone(46)

White powders, yield 35.9%. mp: 121 ~ 122 °C. ¹H NMR (DMSO-*d*₆, 300 MHz) δ : 8.02 (s, 2H), 7.33 (t, *J* = 6.42 Hz, 2H), 7.03 (s, 2H), 6.88 (t, *J* = 5.91 Hz, 2H), 6.78 (d, *J* = 5.37 Hz, 1H), 6.00 (s, 2H), 5.71 (dd, *J* = 3.50 and 8.61 Hz, 1H), 3.82 (s, 7H), 3.71 (s, 3H), 3.27 (dd, *J* = 3.06 and 13.59 Hz, 1H). MS (ESI): 479.47 [M+H]⁺. Anal. calc. for C₂₆H₂₃FN₂O₆: C, 65.27; H, 4.85; N, 5.85. Found: C, 65.26; H, 4.86; N, 5.84.

4.1.36.

(5-(benzo[*d*][1,3]dioxol-5-yl)-3-(3,4,5-trimethoxyphenyl)-4,5-dihydro-1*H*-pyrazol-1-yl)(4-chlorophenyl)methanone(47)

White powders, yield 34.6%. mp: 128 ~ 129 °C. ¹H NMR (DMSO-*d*₆, 300 MHz) δ : 7.97 (d, *J* = 5.61 Hz, 2H), 7.57 (d, *J* = 6.12 Hz, 2H), 7.03 (s, 2H), 6.88 (t, *J* = 5.91 Hz, 2H), 6.79 (d, *J* = 5.55 Hz, 1H), 6.00 (s, 2H), 5.71 (dd, *J* = 2.97 and 8.43 Hz, 1H), 3.82 (s, 7H), 3.71 (s, 3H), 3.27 (dd, *J* = 3.03 and 13.62 Hz, 1H). MS (ESI): 495.92 [M+H]⁺

⁺. Anal. calc. for C₂₆H₂₃ClN₂O₆: C, 53.62; H, 3.97; N, 5.66. Found: C, 53.61; H, 3.96; N, 5.67.

4.2. Biological Assays

4.2.1. Antiproliferation assay [24-26]

A549 human lung cancer cells, MCF-7 human breast cancer cells and HepG-2 human liver cancer cells cultured in DMEM/10% (V/V) fetal bovine serum, in 5% CO₂ water saturated atmosphere at 37 °C. A549, MCF-7 Cell and HepG-2 suspensions (10000/mL) were prepared and 100 µL/well dispensed into 96-well plates (Costar) giving 1000 cells/well respectively. The plates were returned to the incubator for 18 h to allow the cells to reattach. These compounds were initially prepared at 20 mM in DMSO. Aliquots (200 µL) were diluted into 20 mL culture medium giving 200 µM, and 10 serial dilutions of 3×prepared. Aliquots (100 µL) of each dilution were added to the wells, giving doses ranging from 100 µM to 0.005 µM. After a further incubated at 37 °C for 24 h in a humidified atmosphere with 5% CO₂, the cell viability was assessed by the fresh MTT (Sigma, 4 mg/mL in PBS) reduction assay and carried out strictly according to the manufacturer instructions. Each assay was carried out for at least three times. The results were summarized in [Table 3](#).

4.2.2. Tubulin polymerization assay

Bovine brain tubulin was purified as described previously. [27] To evaluate the effect of the compounds on tubulin assembly *in vitro*, varying concentrations of compounds were preincubated with 10 µM bovine brain tubulin in glutamate buffer at 30 °C and then cooled to 0 °C. [28, 29] After the addition of 0.4 mM GTP, the mixtures were transferred to 0 °C cuvettes in a recording spectrophotometer and warmed up to 30 °C. Then, the assembly of tubulin was observed turbidimetrically at 350 nm. The IC₅₀ was defined as the compound concentration that inhibited the extent of assembly by 50% after 20 min incubation..

4.2.3. Annexin-V Assay

Approximately 10⁵ cells HepG-2 cells /well were plated in a 12 well plate and allowed to adhere. After 12 h, the medium was replaced with fresh culture medium

containing compound **18** at final concentrations of 0, 0.01, 0.03 and 0.05 μM . Then cells were harvested after 24 h.

They were trypsinized, washed in PBS and centrifuged at 2000 rpm for 5 min. The pellet was then resuspended in 500 μL of staining solution (containing 5 μL Annexin V-PE and 5 μL PI in Binding Buffer), mixed gently and incubated for 15 min at room temperature (15 - 25°C) in dark. The samples were then read in a FACScalibur flow cytometer (USA) at 488 nm excitation. Analyses were performed by the software supplied in the instrument.

4.2.4. Flow Cytometric Analysis of Cell Cycle Distribution.

For flow cytometric analysis of DNA content, 5×10^5 HepG-2 cells in exponential growth were treated with different concentrations of compound **18** for 48 h. After the incubation, the cells were collected, centrifuged, and fixed with ice-cold ethanol (70%). The cells were treated with lysis buffer containing RNase A and 0.1% Triton X-100 and stained with PI. Samples were analyzed on a Cytomic FC500 flow cytometer (Beckman Coulter). DNA histograms were analyzed using Mod Fit for Windows.

4.3. Molecular docking

Molecular docking of compounds **15-47** into the three dimensional X-ray structure of tubulin (PDB code: 1SA0) was carried out using the Discovery Studio (version 3.5) as implemented through the graphical user interface DS- CDOCKER protocol. [30]

The three-dimensional structures of the aforementioned compounds were constructed using Chem. 3D ultra 12.0 software [Chemical Structure Drawing Standard; Cambridge Soft corporation, USA (2010)], then they were energetically minimized by using MMFF94 with 5000 iterations and minimum RMS gradient of 0.10. The crystal structures of two TS proteins complex were retrieved from the RCSB Protein Data Bank (<http://www.rcsb.org/pdb/home/home.do>). All bound waters and ligands were eliminated from the protein and the polar hydrogen was added to the proteins.

Acknowledgments

The work was financed by a grant (No. J1103512) from National Natural Science Foundation of China and Major Projects on Control and Rectification of Water Body Pollution (No. 2011ZX07204-001-004).

References:

1. C. C. Kuo, H. P. Hsieh, W. Y. Pan, C. P. Chen, J. P. Liou, S. J. Lee, Y. L. Chang, L. T. Chen, C. T. Chen and J. Y. Chang, *Cancer Res.* 64 (2004) 4621-4628.
2. R. Romagnoli, P. G. Baraldi, A. Brancale, A. Ricci, E. Hamel, R. Bortolozzi, G. Basso and G. Viola, *J. Med. Chem.* 54 (2011) 5144-5153.
3. J. Liu, C. H. Zheng, X. H. Ren, F. Zhou, W. Li, J. Zhu, J. G. Lv and Y. J. Zhou, *J. Med. Chem.* 55 (2012) 5720-5733.
4. C. Dumontet and M. A. Jordan, *Nat. Rev. Drug. Discov.* 9 (2010) 790-803.
5. F. Pellegrini and D. R. Budman, *Cancer Invest.* 23 (2005) 264-273.
6. S. Honore, E. Pasquier and D. Braguer, *Cell Mol Life Sci.* 62 (2005) 3039-3056.
7. R. Romagnoli, P. G. Baraldi, M. K. Salvador, D. Preti, T. M. Aghazadeh, A. Brancale, X. H. Fu, J. Li, S. Z. Zhang, E. Hamel, R. Bortolozzi, E. Porcu, G. Basso and G. Viola, *J. Med. Chem.* 55 (2012) 5433-5445.
8. C. M. Lin, H. H. Ho, G. R. Pettit and E. Hamel, *Biochemistry-US* 28 (1989) 6984-6991.
9. G. R. Pettit, M. R. Rhodes, D. L. Herald, E. Hamel, J. M. Schmidt and R. K. Pettit, *J. Med. Chem.* 48 (2005) 4087-4099.
10. D. Y. Kim, K. H. Kim, N. D. Kim, K. Y. Lee, C. K. Han, J. H. Yoon, S. K. Moon, S. S. Lee and B. L. Seong, *J. Med. Chem.* 49 (2006) 5664-5670.
11. Y. J. Li, Y. J. Qin, J. A. Makawana, Y. T. Wang, Y. Q. Zhang, Y. L. Zhang, M. R. Yang, A. Q. Jiang and H. L. Zhu, *Bioorg. Med. Chem.* 2014.
12. R. Romagnoli, P. G. Baraldi, O. Cruz-Lopez, C. C. Lopez, M. D. Carrion, A. Brancale, E. Hamel, L. Chen, R. Bortolozzi, G. Basso and G. Viola, *J. Med. Chem.* 53 (2010) 4248-4258.
13. Ohsumi, K.; Hatanaka, T.; Fujita, K.; Nakagawa, R.; Fukuda, Y.; Nihai, Y.; Suga,

- Y.; Morinaga, Y.; Akiyama, Y.; Tsuji, T.. *Bioorg. Med. Chem. Lett.* 8 (1988) 3153–3158.
14. M. Wu, Q. Sun, C. Yang, D. Chen, J. Ding, Y. Chen, L. Lin and Y. Xie, *Bioorg. Med. Chem. Lett.* 17 (2007) 869-873.
15. G. R. Pettit, C. R. Anderson, D. L. Herald, M. K. Jung, D. J. Lee, E. Hamel and R. K. Pettit, *J. Med. Chem.* 46 (2003) 525-531.
16. S. K. Tahir, E. K. Han, B. Credo, H. S. Jae, J. A. Pietenpol, C. D. Scatena, J. R. Wu-Wong, D. Frost, H. Sham, S. H. Rosenberg and S. C. Ng, *Cancer Res.* 61 (2001) 5480-5485.
17. Y. Lu, C. M. Li, Z. Wang, C. N. Ross, J. Chen, J. T. Dalton, W. Li and D. D. Miller, *J. Med. Chem.* 52 (2009) 1701-1711.
18. R. LeBlanc, J. Dickson, T. Brown, M. Stewart, H. N. Pati, D. VanDerveer, H. Arman, J. Harris, W. Pennington, H. J. Holt and M. Lee, *Bioorg. Med. Chem.* 13 (2005) 6025-6034.
19. M. Xiao, S. Ahn, J. Wang, J. Chen, D. D. Miller, J. T. Dalton and W. Li, *J. Med. Chem.* 56 (2013) 3318-3329.
20. X. H. Yang, Q. Wen, T. T. Zhao, J. Sun, X. Li, M. Xing, X. Lu and H. L. Zhu, *Bioorg. Med. Chem.* 20 (2012) 1181-1187.
21. C. Y. Li, Q. S. Li, L. Yan, X. G. Sun, R. Wei, H. B. Gong and H. L. Zhu, *Bioorg. Med. Chem.* 20 (2012) 3746-3755.
22. I. Vermes, C. Haanen, H. Steffens-Nakken and C. Reutelingsperger, *J. Immunol. Methods* 184 (1995) 39-51.
23. M. N. Aboul-Enein, A. A. El-Azzouny, M. I. Attia, Y. A. Maklad, K. M. Amin, M. Abdel-Rehim and M. F. El-Behairy, *Eur. J. Med. Chem.* 47 (2012) 360-369.
24. Z. Hou, I. Nakanishi, T. Kinoshita, Y. Takei, M. Yasue, R. Misu, Y. Suzuki, S. Nakamura, T. Kure, H. Ohno, K. Murata, K. Kitaura, A. Hirasawa, G. Tsujimoto, S. Oishi and N. Fujii, *J. Med. Chem.* 55 (2012) 2899-2903.
25. Q. S. Li, C. Y. Li, X. Lu, H. Zhang and H. L. Zhu, *Eur. J. Med. Chem.* 50 (2012) 288-295.
26. R Romagnoli, P. G. Baraldi, M. K. Salvador, D. Preti, M. A. Tabrizi, A. Brancale,

- X. H. Fu, J. Li, S. Z. Zhang, E. Hamel, R. Bortolozzi, E. Porc, G. Basso, and G. Viola, *J. Med Chem.* (55) 2012, 5433–5445.
27. E. Hamel and C. M. Lin, *Biochemistry-Us* 23 (1984) 4173-4184.
28. E. Hamel, *Cell Biochem Biophys* 38 (2003) 1-22.
29. Y. Luo, K. M. Qiu, X. Lu, K. Liu, J. Fu and H. L. Zhu, *Bioorg. Med. Chem.* 19 (2011) 4730-4738.
30. G. Wu, D. H. Robertson, C. R. Brooks and M. Vieth, *J. Comput. Chem.* 24 (2003) 1549-1562.

Figure captions:

Figure 1 Inhibitors and Potential Inhibitors of Tubulin Polymerization

Figure 2 Crystal structure diagram of compound **23**. H atoms are shown as small spheres of arbitrary radii.

Figure 3 Representative flow cytometric histograms of apoptotic HepG-2 cells after 24 h treatment with compound **18**. The cells were harvested and labeled with Annexin-V-FITC and PI and then analyzed by flow cytometry.

Figure 4 Effects of compound **18** on cell cycle progression of HepG-2 cells were determined by flow cytometry analysis. HepG-2 cells were treated with different concentrations of compound **18** for 48 h. The percentage of cells in each cycle phase was indicated.

Figure 5 The CDOCKER_INTERACTION_ENERGY (kcal/mol) obtained from the docking study of compounds **15-47** by the CDOCKER protocol (Discovery Studio 3.5, Accelrys, Co. Ltd). It is clear that compound **18**, showed lowest interaction energy of all the synthesized compounds and the interaction energy reached up to -60.69 kcal/mol.

Figure 6 The binding mode between the active conformation of compound **18** and the target protein tubulin (PDB code: 1SA0) provided by the CDOCKER protocol (Discovery Studio 3.5, Accelrys, Co. Ltd). We employed 2D diagram (**Figure 6A**), 3D interaction map (**Figure 6B**) to display the interaction between **18** and the targeted protein. In the binding model, compound **18** is nicely bound to tubulin via four hydrogen bonds.

Figure 7 The surface model structure to display the interaction between compound **18** and the targeted protein tubulin.

Scheme 1 General synthesis of compounds **15 - 37**.

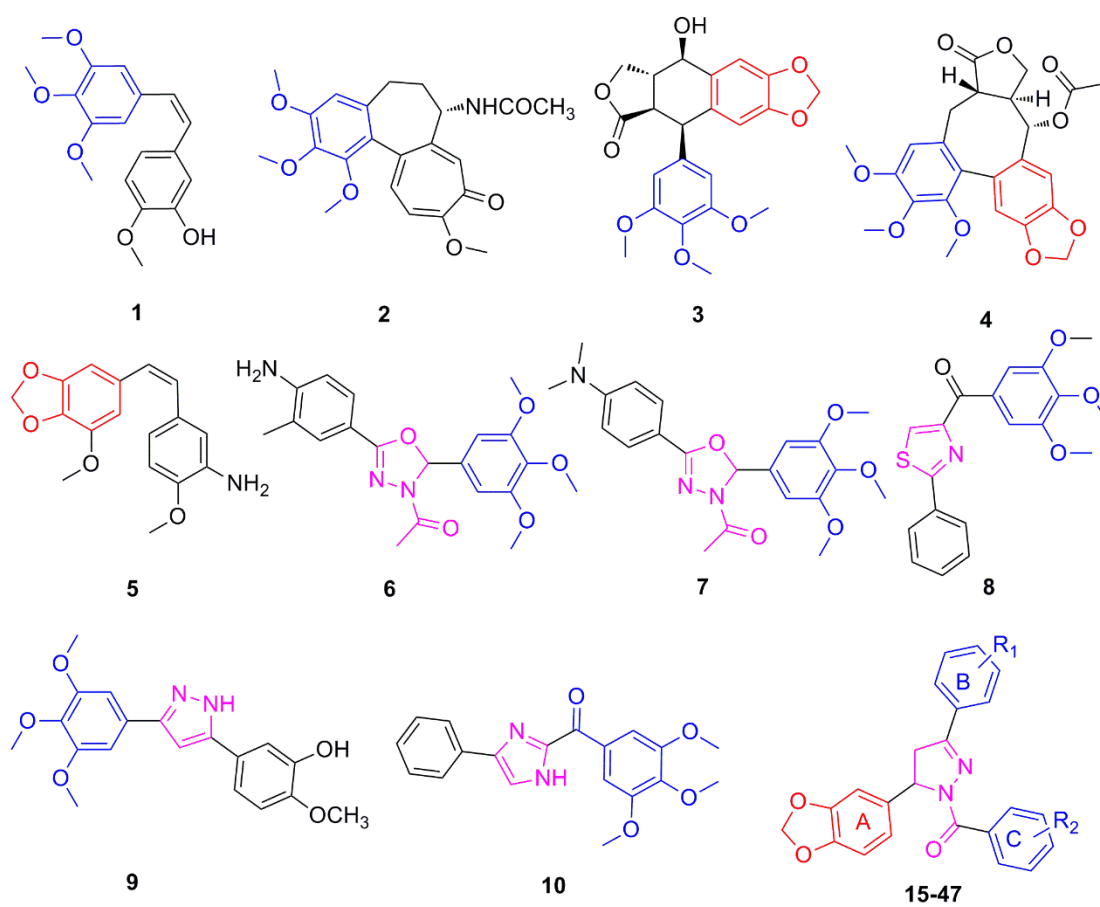


Figure 1. Inhibitors and Potential Inhibitors of Tubulin Polymerization.

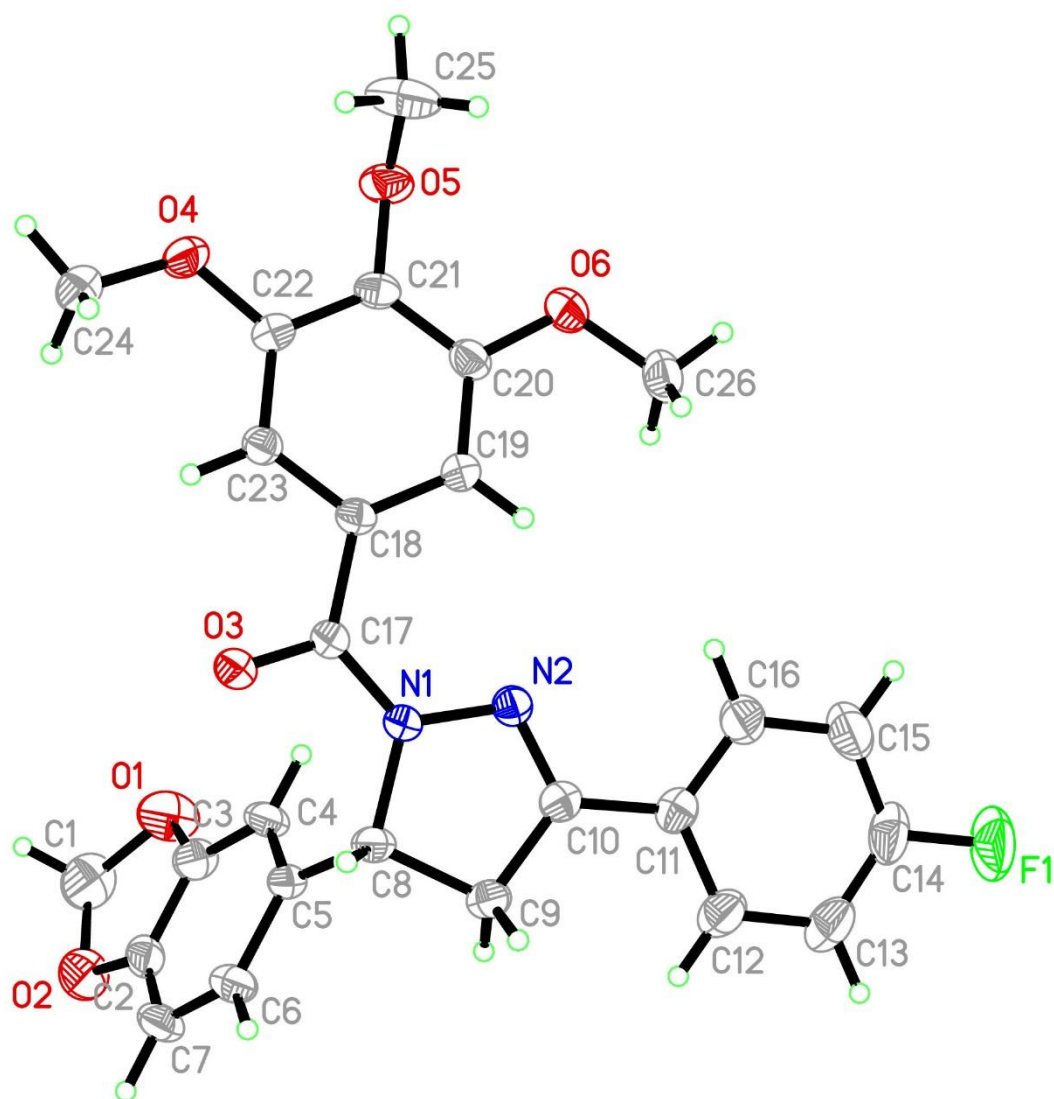


Figure 2. Crystal structure diagram of compound **23**. H atoms are shown as small spheres of arbitrary radii.

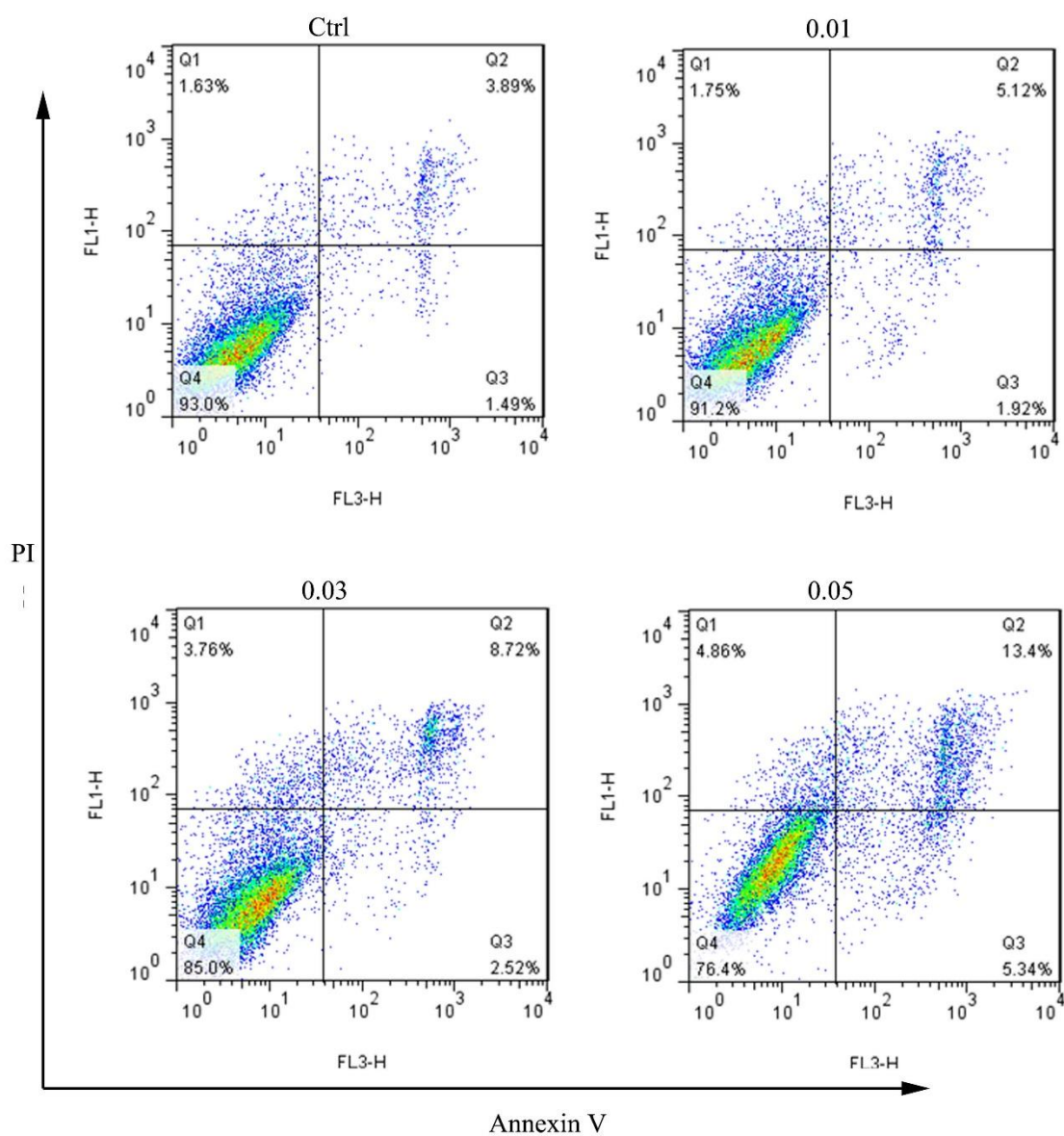


Figure 3. Representative flow cytometric histograms of apoptotic HepG-2 cells after 24 h treatment with compound **18**. The cells were harvested and labeled with Annexin-V-FITC and PI and then analyzed by flow cytometry.

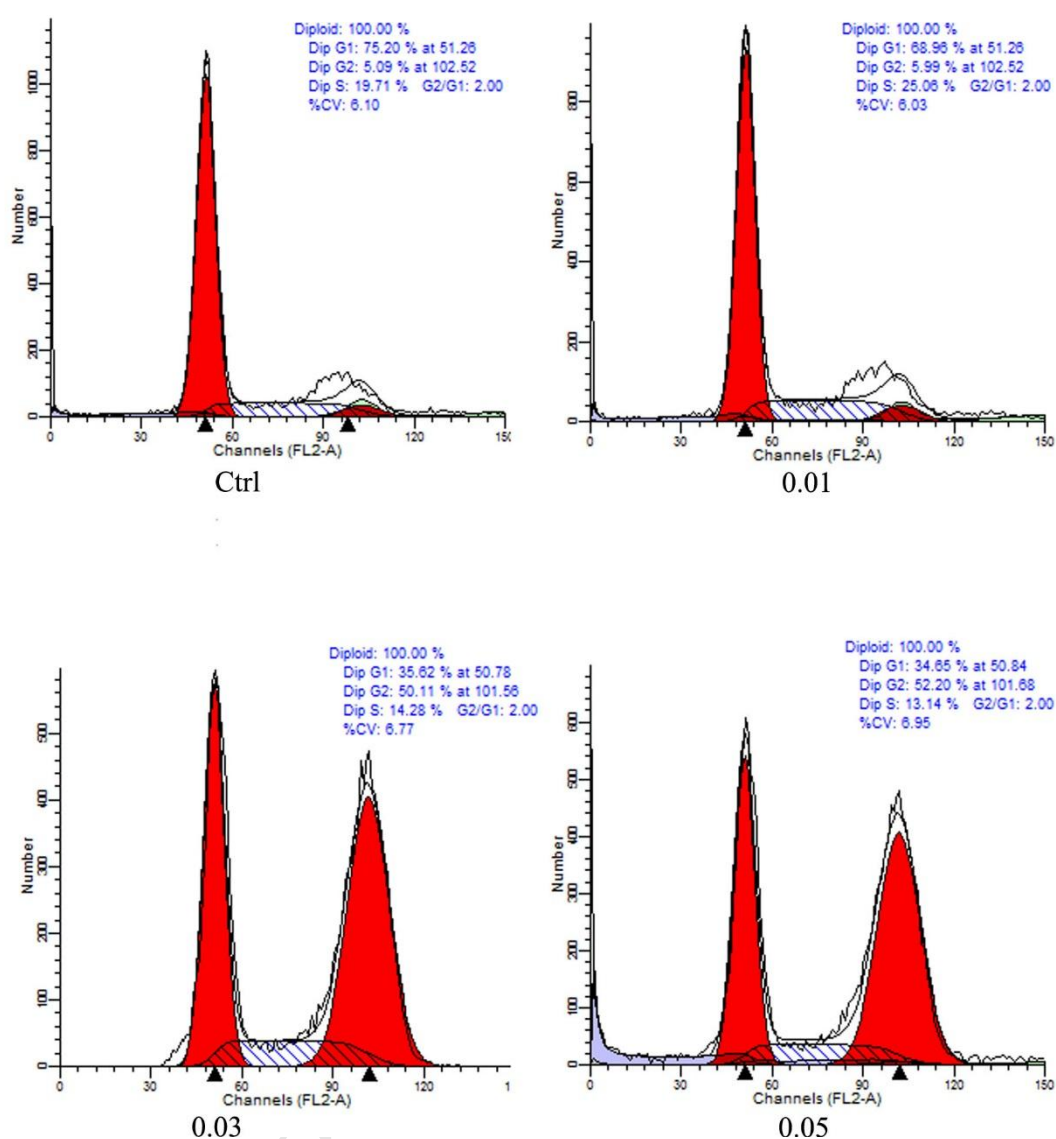


Figure 4. Effects of compound **18** on cell cycle progression of HepG-2 cells were determined by flow cytometry analysis. HepG-2 cells were treated with different concentrations of compound **18** for 48 h. The percentage of cells in each cycle phase was indicated.

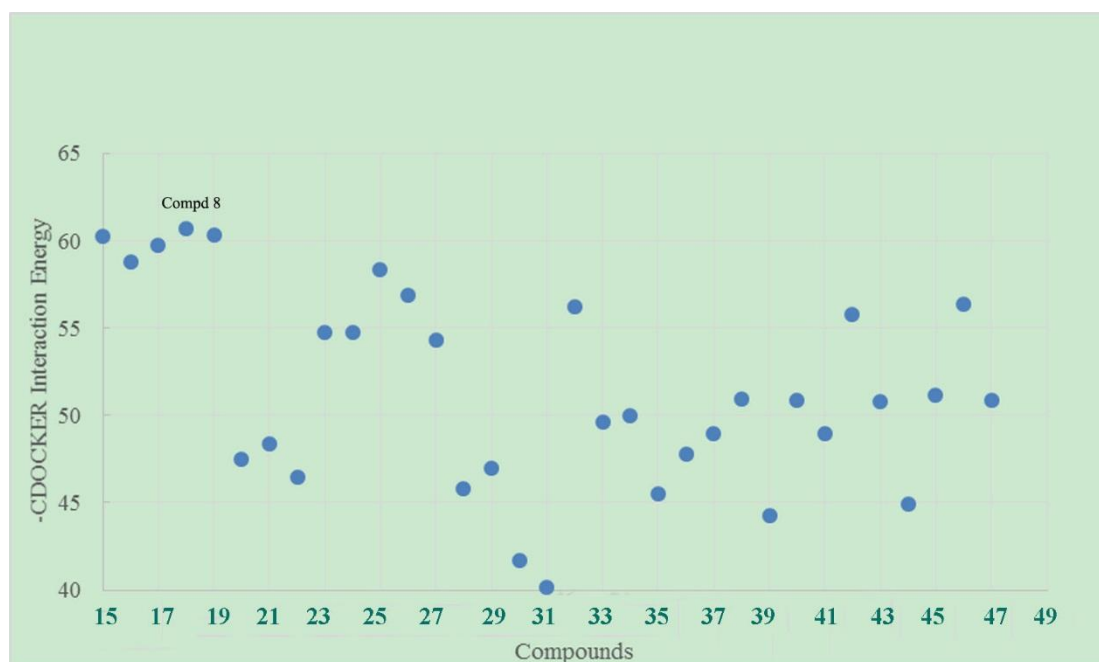


Figure 5. The CDOCKER_INTERACTION_ENERGY (kcal/mol) obtained from the docking study of compounds **15-47** by the CDOCKER protocol (Discovery Studio 3.5, Accelrys, Co. Ltd). It is clear that compound **18**, showed lowest interaction energy of all the synthesized compounds and the interaction energy reached up to -60.69 kcal/mol.

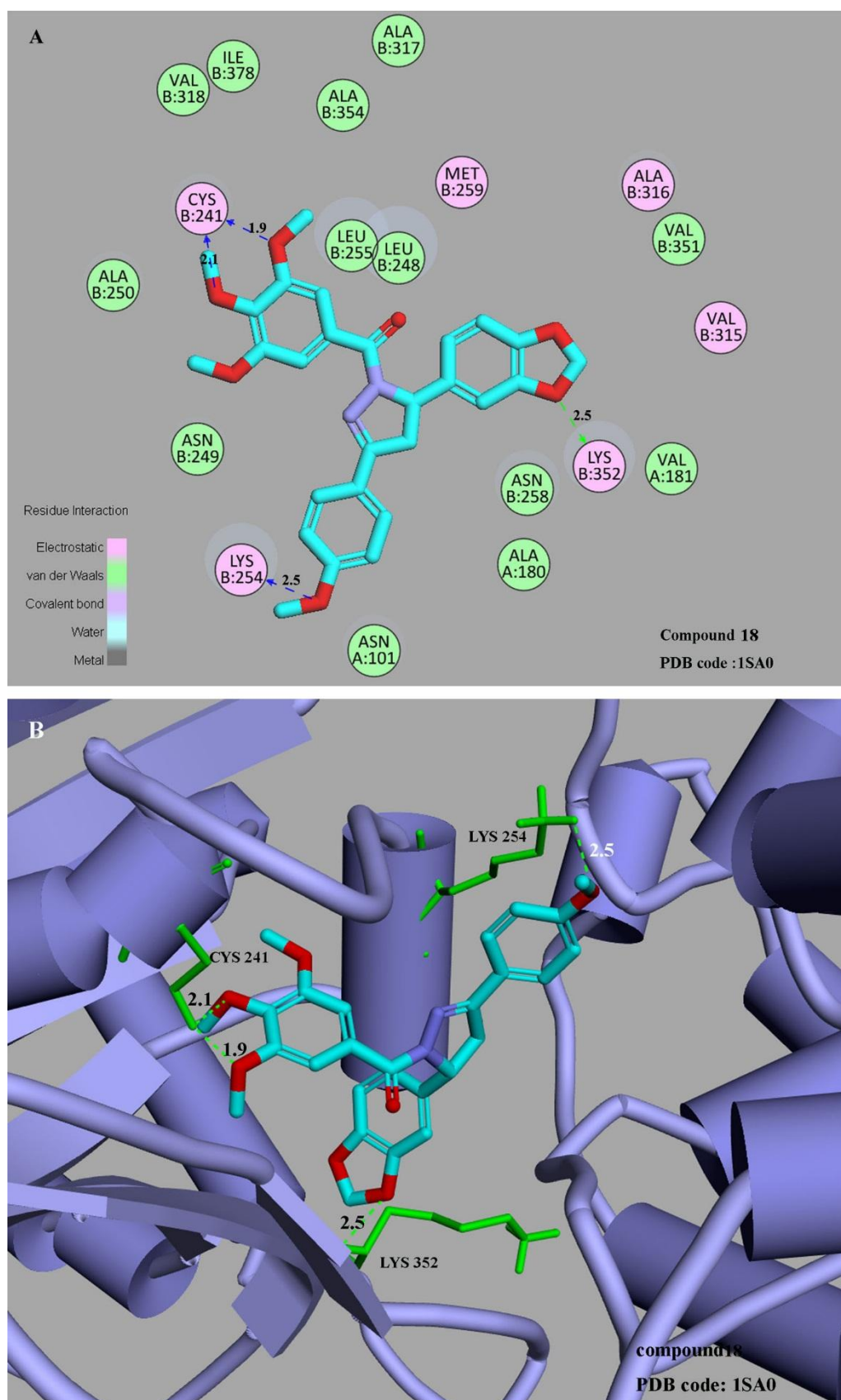


Figure 6 The binding mode between the active conformation of compound **18** and the target protein tubulin (PDB code: 1SA0) provided by the CDOCKER protocol

(Discovery Studio 3.5, Accelrys, Co. Ltd). We employed 2D diagram (**Figure 6A**), 3D interaction map (**Figure 6B**) to display the interaction between **18** and the targeted protein. In the binding model, compound **18** is nicely bound to tubulin via four hydrogen bonds.

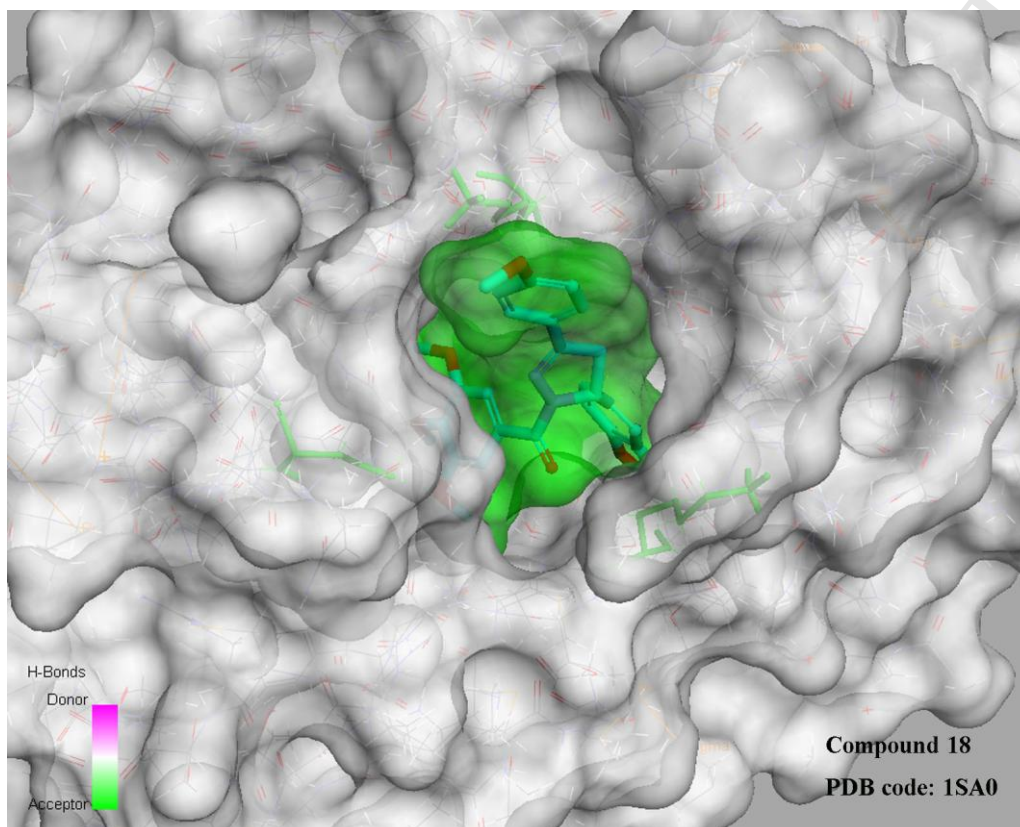
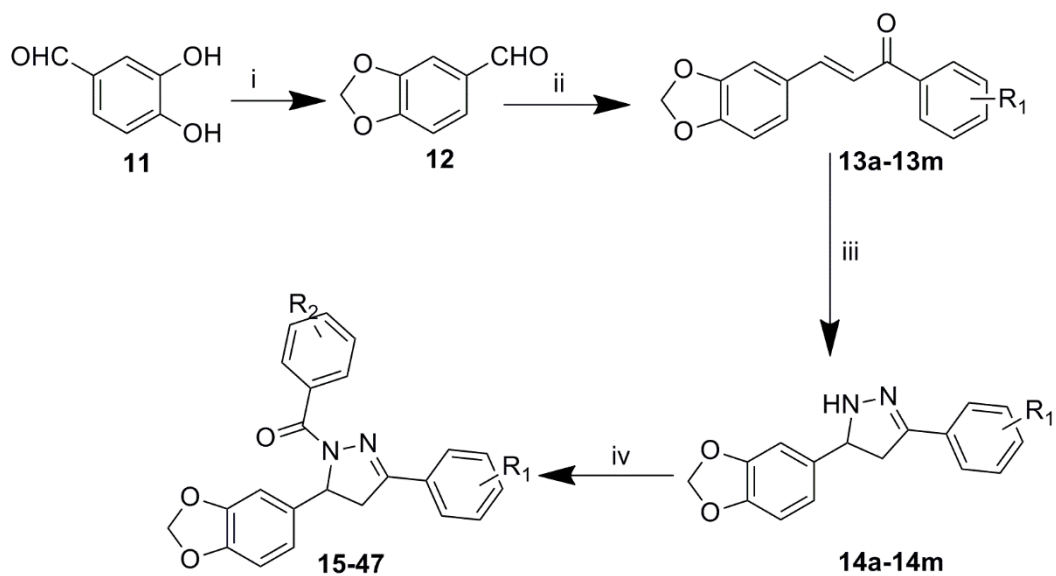
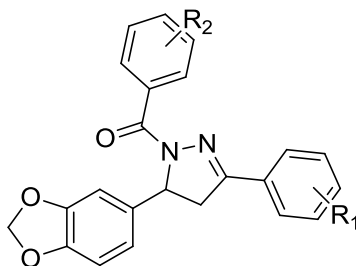


Figure 7. The surface model structure to display the interaction between compound **18** and the targeted protein tubulin.



Scheme 1. General synthesis of compounds **15 - 47**. Reagents and conditions: (i) CH_2Cl_2 , K_2CO_3 , DMF, reflux; (ii) EtOH, NaOH, r.t.; (iii) $\text{NH}_2\cdot\text{NH}_2\cdot\text{H}_2\text{O}$, EtOH, reflux; (iv) EDC·HCl, HOBT, CH_2Cl_2 , reflux.

Table 1 Structure of compounds **15-47**

compounds	R ₁	R ₂	compounds	R ₁	R ₂
15	4-OCH ₂ CH ₃	3,4,5-(OCH ₃) ₃	32	3,4-(OCH ₃) ₂	4-Br
16	2-OCH ₃	3,4,5-(OCH ₃) ₃	33	3,4,5-(OCH ₃) ₃	4-Br
17	3-OCH ₃	3,4,5-(OCH ₃) ₃	34	4-Br	4-Br
18	4-OCH ₃	3,4,5-(OCH ₃) ₃	35	4-Cl	4-Br
19	3,4-(OCH ₃) ₂	3,4,5-(OCH ₃) ₃	36	4-F	4-Br
20	3,4,5-(OCH ₃) ₃	3,4,5-(OCH ₃) ₃	37	4-CH ₃	4-Br
21	4-Br	3,4,5-(OCH ₃) ₃	38	3-CH ₃	4-Br
22	4-Cl	3,4,5-(OCH ₃) ₃	39	H	4-Br
23	4-F	3,4,5-(OCH ₃) ₃	40	4-OCH ₃	4-F
24	3- Cl	3,4,5-(OCH ₃) ₃	41	4-OCH ₃	4-Cl
25	4-CH ₃	3,4,5-(OCH ₃) ₃	42	4-OCH ₃	3-OCH ₃
26	3-CH ₃	3,4,5-(OCH ₃) ₃	43	4-OCH ₃	4-OCH ₃
27	H	3,4,5-(OCH ₃) ₃	44	4-OCH ₃	3,4-(OCH ₃) ₂
28	4-OCH ₂ CH ₃	4-Br	45	4-OCH ₃	H
29	2-OCH ₃	4-Br	46	3,4,5-OCH ₃	4-F
30	3-OCH ₃	4-Br	47	3,4,5-OCH ₃	4-Cl
31	4-OCH ₃	4-Br			

Table 2. Crystallographical and experimental data for compound **23**

Compound	23
Empirical formula	C ₂₆ H ₂₃ FN ₂ O ₆
Formula weight	478.47
Crystal system	Triclinic
Space group	P-1
<i>a</i> (Å)	17.8041(17)
<i>b</i> (Å)	6.6099(6)
<i>c</i> (Å)	20.616(2)
<i>a</i> (°)	90.00
<i>b</i> (°)	109.900(3)
<i>c</i> (°)	90.00
<i>V</i> (Å ³)	2281.3(4)
<i>Z</i>	38
D _{calc} /g cm ⁻³	1.716
<i>h</i> range (°)	3.26-27.48
F(000)	1178
Reflections collected/unique	22467/5190
Data/restraints/parameters	5190/0/319
Absorption coefficient (mm ⁻¹)	0.193
R1; wR2 [<i>I</i> > 2σ(<i>I</i>)]	0.0536/0.1125
R1; wR2 (all data)	0.0934/0.1291
GOF	1.023

Table 3. *In vitro* Inhibition of Tubulin Polymerization and anticancer activities.

Compds	IC ₅₀ ±SD (μM)			
	A549 ^a	MCF-7 ^a	HepG-2 ^a	Tubulin ^b
15	0.09 ± 0.02	0.17 ± 0.20	0.07 ± 0.02	2.19 ± 0.12
16	0.11 ± 0.01	0.21 ± 0.14	0.12 ± 0.05	2.35 ± 0.13
17	0.09 ± 0.03	0.06 ± 0.04	0.07 ± 0.03	1.91 ± 0.06
18	0.07 ± 0.01	0.05 ± 0.004	0.03 ± 0.009	1.88 ± 0.07
19	0.08 ± 0.02	0.07 ± 0.03	0.06 ± 0.10	2.13 ± 0.11
20	2.23 ± 0.11	3.26 ± 0.09	3.15 ± 0.08	11.37 ± 0.28
21	4.21 ± 0.09	6.37 ± 0.17	5.25 ± 0.15	19.45 ± 0.56
22	3.08 ± 0.03	4.26 ± 0.12	3.16 ± 0.04	18.02 ± 0.54
23	0.76 ± 0.09	0.32 ± 0.11	0.25 ± 0.09	7.89 ± 0.21
24	7.11 ± 0.11	9.23 ± 0.13	7.15 ± 0.09	>40
25	1.14 ± 0.04	2.35 ± 0.05	2.91 ± 0.09	10.11 ± 0.45
26	5.08 ± 0.09	7.34 ± 0.12	5.17 ± 0.11	7.08 ± 0.32
27	2.19 ± 0.03	3.38 ± 0.05	2.24 ± 0.12	15.63 ± 0.91
28	>10	>10	>10	>40
29	>10	>10	>10	>40
30	>10	>10	>10	>40
31	>10	>10	>10	>40
32	3.19 ± 0.09	4.46 ± 0.12	6.26 ± 0.13	22.06 ± 0.78
33	4.16 ± 0.04	5.26 ± 0.11	6.22 ± 0.06	25.06 ± 0.95
34	>10	>10	>10	>40
35	>10	>10	>10	>40
36	2.45 ± 0.04	5.11 ± 0.12	>10	>40
37	>10	>10	>10	>40
38	>10	>10	>10	>40
39	>10	>10	>10	>40
40	1.08 ± 0.12	1.77 ± 0.09	1.86 ± 0.13	7.69 ± 0.42
41	7.14 ± 0.24	8.66 ± 0.31	8.38 ± 0.12	>40
42	6.17 ± 0.14	8.22 ± 0.13	6.25 ± 0.14	34.77 ± 0.42
43	4.08 ± 0.06	6.41 ± 0.08	5.05 ± 0.12	25.79 ± 1.04

44	2.73 ± 0.06	3.56 ± 0.05	3.77 ± 0.08	15.73 ± 0.77
45	5.21 ± 0.08	5.37 ± 0.17	6.25 ± 0.07	35.45 ± 1.05
46	0.78 ± 0.02	0.22 ± 0.03	1.06 ± 0.10	2.09 ± 0.05
47	4.26 ± 0.11	4.77 ± 0.13	2.14 ± 0.09	21.73 ± 0.33
CA-4^c	0.14 ± 0.06	0.31 ± 0.08	0.17 ± 0.03	2.1 ± 0.12

All experiments were independently performed at least three times.

^a Cancer cells were purchased from NanJing KeyGen Biotech Co.,Ltd., which subcultured by State Key Laboratory of Pharmaceutical Biotechnology, Nanjing University all of which; A549 (human lung cancer cells), SW480 (human colon cancer cells) and MCF-7 (human breast cancer cells).

^b Inhibition of tubulin polymerization.

^c Used as a positive control.

- > 32 novel Pyrazoline-containing derivatives has been designed and synthesized.
- > Crystal structure of compound **23** was determined.
- > Their biological activities were tested as potential tubulin assembling inhibitors.
- > The docking model were established and analyzed.
- > Compound **18** displayed the most potent antitumor activity.

ACCEPTED MANUSCRIPT

Supplementary material

Design, Synthesis and Biological Evaluation of Novel Pyrazoline-Containing Derivatives as Potential Tubulin Assembling Inhibitors

Ya-Juan Qin^{a†}, Yu-jing Li^{a†}, Ai-Qin Jiang^{b*}, Meng-Ru Yang^a, Qi-Zhang Zhu^a,
Hong-Dong^{a*}, Hai-Liang Zhu^{a*}

^a *State Key Laboratory of Pharmaceutical Biotechnology, School of Life Science,
Nanjing University, Nanjing 210093, P. R. China*

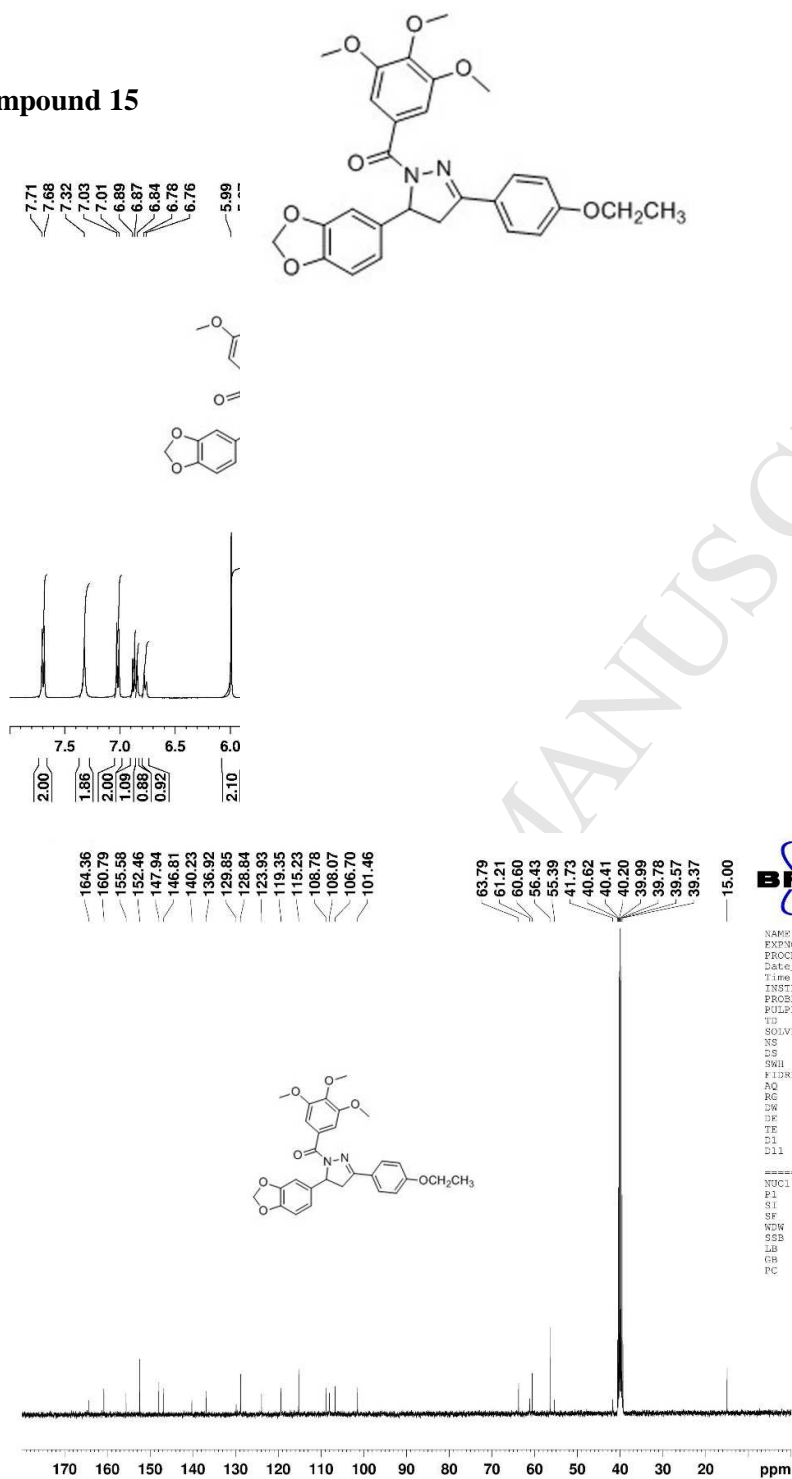
^b *School of Medicine, Nanjing University, Nanjing 210093, P. R. China*

[†] Both authors contributed equally to this work.

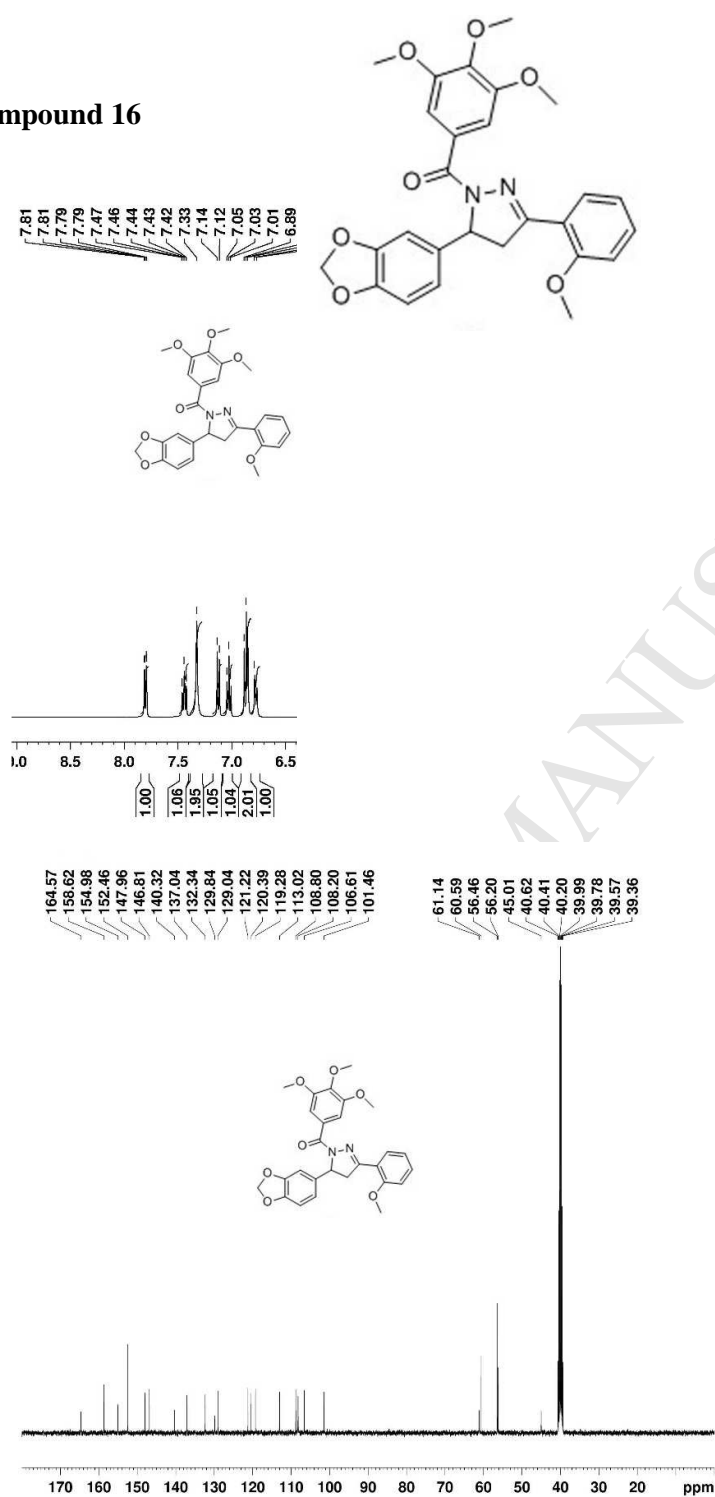
Contents

Compounds **15, 16, 20, 21, 29, 34**

Compound 15



Compound 16



```

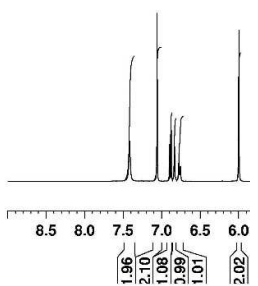
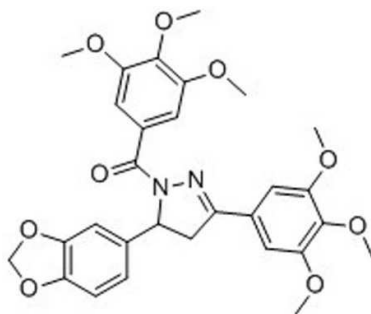
NAME      1024
EXPNO     81
PROCNO    1
Date_     20141024
Time      9.50
INSTRUM   spect
PROBHD    5 mm BBOBO BB-
PULPROG   zgpg30
ID         65536
SOLVENT   DMSO
NS         256
DS         4
SWH        24038.461 Hz
FIDRES     0.366798 Hz
AQ         1.3631988 sec
RG         203
DW         20.800 usec
DE         6.50 usec
TE         298.4 K
D1         2.0000000 sec
D11        0.0300000 sec

----- CHANNEL f1 -----
NUC1      13C
P1        9.19 usec
SI        32768
SF        100.6032250 MHz
WDW       EM
GB        0
IR        1.00 Hz
SB        0
FC        1.40

```

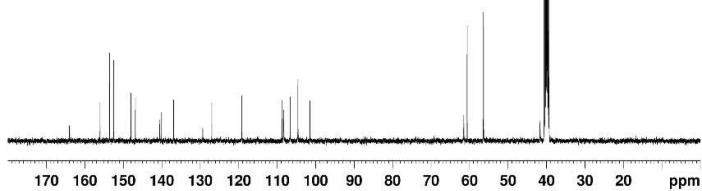
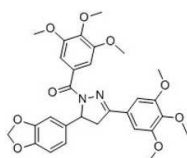
Compound 20

7.42
7.06
6.80
6.88
6.84
6.78
6.76
6.00
5.74



164.00
156.01
153.52
152.50
147.97
146.83
140.46
140.02
136.93
129.37
127.02
119.24
108.80
108.29
106.58
104.60
101.48

61.51
60.63
56.41
56.35
41.67
40.60
40.39
40.18
39.97
39.76
39.56
39.35



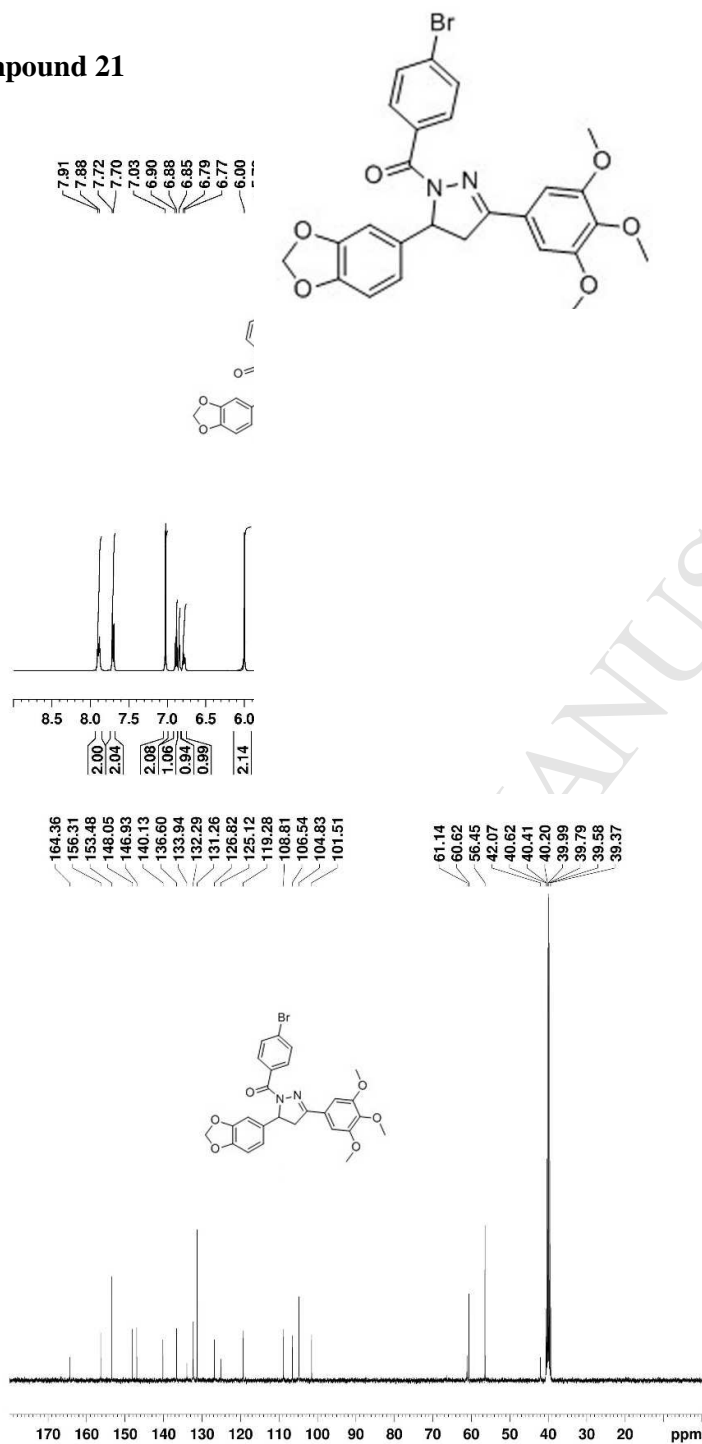
```

NAME          1024
EXPNO         84
PROCNO        1
Date_         20141024
Time          10.55
INSTRUM       spect
PROBHD        5 mm PABBO BB-
PULPROG       zgpg30
TD            65536
SOLVENT       DMSO
NS            1024
DS            4
SWH           24038.461 Hz
FIDRES        0.366798 Hz
AQ            1.3631988 sec
RG            203
DW            20.800 usec
DE            6.50 usec
TE            298.1 K
D1            2.00000000 sec
D11           0.03000000 sec

===== CHANNEL f1 =====
NUC1          13C
P1            9.19 usec
SI            32768
SF            100.6052250 MHz
WDW           EM
SSB           0
LB            1.00 Hz
GB            0
PC            1.40

```

Compound 21



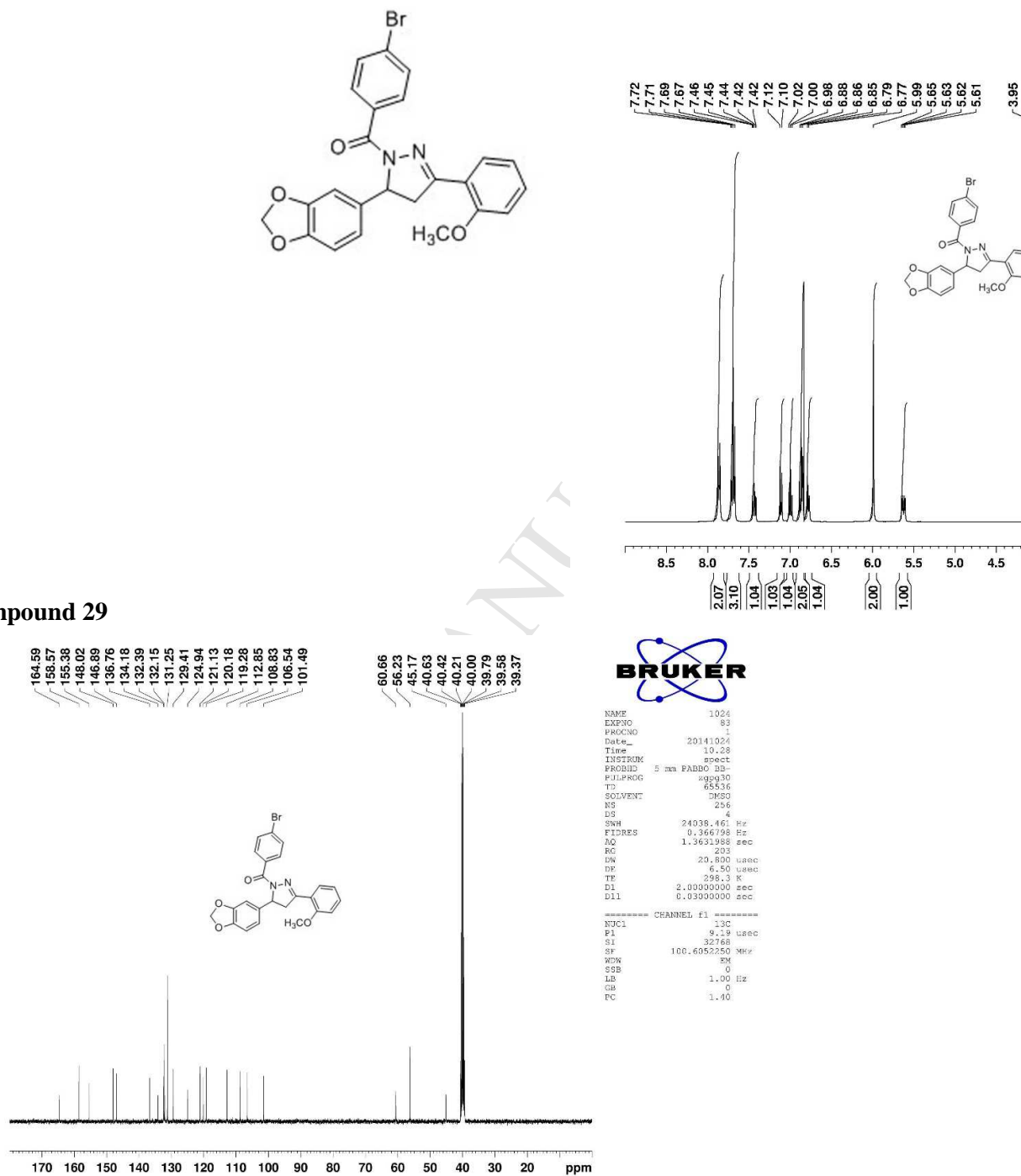
```

NAME          0508
EXPNO         60
PROCNO        1
Date_         20140508
Time          14.53
INSTRUM       spect
PROBHD        5 mm PABBO BB-
PULPROG       zgpg30
TD            65536
SOLVENT       DMSO
NS            256
DS            4
SWH           24038.461 Hz
FIDRES        0.366798 Hz
AQ            1.3631988 sec
RG            203
AQ            20.800 usec
DE            6.50 usec
TE            300.2 K
D1            2.0000000 sec
D11           0.0300000 sec

===== CHANNEL f1 =====
NUC1          13C
P1            9.19 usec
S1            32768
SF            100.6052250 MHz
WDW           EM
SSB           0
LB            1.00 Hz
GB            0
PC            1.40

```

Compound 29



Compound 34

